



uOttawa

L'Université canadienne
Canada's university

FACULTÉ DES ÉTUDES SUPÉRIEURES
ET POSTDOCTORALES



FACULTY OF GRADUATE AND
POSTDOCTORAL STUDIES

Puneet Dargar

AUTEUR DE LA THÈSE / AUTHOR OF THESIS

M.A.Sc. (Mechanical Engineering)

GRADE / DEGREE

Department of Mechanical Engineering

FACULTÉ, ÉCOLE, DÉPARTEMENT / FACULTY, SCHOOL, DEPARTMENT

Effect of Surfactants on the Hydrodynamics of Bubble Columns and Three-Phase Fluidized Beds

TITRE DE LA THÈSE / TITLE OF THESIS

Yue Chen

DIRECTEUR (DIRECTRICE) DE LA THÈSE / THESIS SUPERVISOR

Arturo Macchi

CO-DIRECTEUR (CO-DIRECTRICE) DE LA THÈSE / THESIS CO-SUPERVISOR

EXAMINATEURS (EXAMINATRICES) DE LA THÈSE / THESIS EXAMINERS

Christopher Lan

Jason Zhang

Gary W. Slater

LE DOYEN DE LA FACULTÉ DES ÉTUDES SUPÉRIEURES ET POSTDOCTORALES /
DEAN OF THE FACULTY OF GRADUATE AND POSTDOCTORAL STUDIES

Effect of Surfactants on the Hydrodynamics of Bubble Columns and
Three-Phase Fluidized Beds

By

Puneet Dargar

Thesis submitted to the
Faculty of Graduate and Postdoctoral Studies
In partial fulfillment of the requirements
For the Master of Applied Science in Chemical Engineering

Department of Chemical Engineering
Univeristy of Ottawa

©Puneet Dargar, Ottawa, Canada, 2005



Library and
Archives Canada

Bibliothèque et
Archives Canada

Published Heritage
Branch

Direction du
Patrimoine de l'édition

395 Wellington Street
Ottawa ON K1A 0N4
Canada

395, rue Wellington
Ottawa ON K1A 0N4
Canada

Your file *Votre référence*

ISBN: 0-494-11249-2

Our file *Notre référence*

ISBN: 0-494-11249-2

NOTICE:

The author has granted a non-exclusive license allowing Library and Archives Canada to reproduce, publish, archive, preserve, conserve, communicate to the public by telecommunication or on the Internet, loan, distribute and sell theses worldwide, for commercial or non-commercial purposes, in microform, paper, electronic and/or any other formats.

The author retains copyright ownership and moral rights in this thesis. Neither the thesis nor substantial extracts from it may be printed or otherwise reproduced without the author's permission.

AVIS:

L'auteur a accordé une licence non exclusive permettant à la Bibliothèque et Archives Canada de reproduire, publier, archiver, sauvegarder, conserver, transmettre au public par télécommunication ou par l'Internet, prêter, distribuer et vendre des thèses partout dans le monde, à des fins commerciales ou autres, sur support microforme, papier, électronique et/ou autres formats.

L'auteur conserve la propriété du droit d'auteur et des droits moraux qui protègent cette thèse. Ni la thèse ni des extraits substantiels de celle-ci ne doivent être imprimés ou autrement reproduits sans son autorisation.

In compliance with the Canadian Privacy Act some supporting forms may have been removed from this thesis.

Conformément à la loi canadienne sur la protection de la vie privée, quelques formulaires secondaires ont été enlevés de cette thèse.

While these forms may be included in the document page count, their removal does not represent any loss of content from the thesis.

Bien que ces formulaires aient inclus dans la pagination, il n'y aura aucun contenu manquant.


Canada

Abstract

Most hydrodynamic correlations and models used for gas-liquid-solid fluidized beds implicitly assume that the major physical properties of the liquid (density, viscosity and surface tension) are sufficient to characterize bubble dynamics. While this is true for pure liquids, multi-component liquids require additional properties due to surface-active agents preferentially accumulating at the gas-liquid interface. Experiments were first conducted to evaluate the effects of surface-active agents (alcohols as well as commercial anionic, cationic and non-ionic surfactants) on the phase holdups and minimum liquid fluidization velocities in a fluidized bed composed of air, water and glass beads of 1.2 and 5 mm in diameter. The gas-liquid interfacial behaviour of the liquid solutions was then characterized by measuring the foamability as well the dynamic surface tension and dilatational surface elasticity using the maximum pressure bubble method. The presence of surface-active agents decreases the minimum liquid fluidization velocity and the effect is more important for the larger particles. The effect of surfactants on the bed phase holdups, and in particular the gas holdup, is significant and more pronounced in the coalesced bubble flow regime where foaming occurred. Further, the bed gas holdups are lower than those observed in the freeboard. The widely used gas holdup correlations proposed by Han et al. (1990) and Larachi et al. (2001) failed. Furthermore, the approach of Gorowara and Fan (1990) which uses the dynamic surface tension also failed as all surfactant solutions present similar phase holdups despite very different surface tension behaviour. More fundamental work is required to elucidate the complex relationship between the physical properties of a multi-component liquid, the degree of bubble coalescence and the hydrodynamic features of multiphase reactors.

Sommaire

La plupart des corrélations et modèles hydrodynamiques utilisés pour les lits fluidisés gaz-liquide-solide supposent implicitement que les propriétés physiques principales du liquide (densité, viscosité et tension superficielle) sont suffisantes pour caractériser la dynamique des bulles. Bien que cela vaille pour les liquides purs, ceux à composants multiples exigent des propriétés additionnelles dues aux agents tensioactifs s'accumulant préférentiellement à l'interface gaz-liquide. Des expériences ont été alors entreprises pour évaluer les effets des agents tensioactifs (alcools et agents tensioactifs anioniques, cationiques et non ioniques commerciaux) sur les retentions de phases et vitesses minimum de fluidisation d'un système composé d'air, eau et billes de verre de 1.2 et 5 millimètres de diamètre. Par la suite, le comportement à l'interface gaz-liquide a été caractérisé en mesurant la capacité de moussage ainsi que la tension superficielle dynamique du liquide en utilisant la méthode de pression maximum de bulle. La présence d'agents tensioactifs diminue la vitesse minimum de fluidisation et l'effet est plus important pour les plus grandes particules. L'effet des agents tensioactifs sur les rétentions de phases, et en particulier la rétention du gaz, est significatif et plus prononcé dans le régime de bulles coalescents. De plus, les rétentions du gaz dans le lit sont plus faibles que celles observées au-dessus du lit. Les corrélations de retentions de gaz les plus utilisées, celles proposées par Han et al. (1990) et Larachi et al. (2001), ont malheureusement échoué. De plus, l'approche de Gorowara et de Fan (1990) qui emploient la tension superficielle dynamique a également échoué puisque toutes les solutions d'agent tensioactif présentent des rétentions de phases semblables en dépit d'un comportement très différent de tension superficielle. Un travail plus fondamental est exigé pour élucider le rapport complexe entre les propriétés physiques d'un liquide à composants multiples, le degré de coalescence de bulles et les paramètres hydrodynamiques des réacteurs multiphasés.

Table of contents

Abstract.....	ii
Sommaire.....	iii
Table of contents	iv
List of tables	v
List of figures.....	vi
Acknowledgements	viii
1. Introduction	1
1.1 Surfactants and their effects on bubble dynamics	3
1.2 Approaches to model phase holdups in the presence of surfactants.....	6
1.3 Thesis objectives and outline.....	7
2. Experimental system and measurement techniques	8
2.1 Multiphase fluidization system.....	8
2.2 Liquid phase characterization.....	9
2.2.1 Surface tension.....	9
2.2.2 Dilatational elasticity	11
2.2.3 Foam retention and half-life times.....	12
2.2.4 Liquid categorization proposed by Gorowara and Fan (1990).....	12
2.3 Hydrodynamic parameters.....	16
2.3.1 Phase holdups	16
2.3.2 Minimum liquid fluidization velocity.....	18
3. Selection of surface-active agents and operating conditions.....	20
3.1. Selection of surface-active agents in aqueous solutions.....	20
3.2. Selection of operating conditions	22
4. Results and discussions	24
4.1 Characterization of liquid physical properties.....	24
4.1.1 Surface tension.....	24
4.1.2 Foam retention and half-life times.....	26
4.2. Bubble column hydrodynamics	28
4.2.1 Gas holdup	28
4.2.2 Correlation of gas holdup data.....	31
4.3. Three-phase fluidized bed hydrodynamics.....	37
4.3.1 Overall phase holdups.....	37
4.3.1.1 Small glass beads ($d_p = 1.2$ mm)	37
4.3.1.2 Large glass beads ($d_p = 5$ mm)	43
4.3.1.3 Summary of effects of selected surface-active agents.....	50
4.3.2 Correlation of phase holdup data.....	53
4.3.3 Minimum liquid fluidization velocity.....	60
5. General conclusions and recommendations	64
Nomenclature.....	66

List of tables

Table 3.1: Selection of surface-active agents.	22
Table 4.1: Analysis of surface tension data according to Gorowara and Fan (1990).....	26
Table 4.2: Applicable range of the Luo et al. (1999) gas holdup correlation.....	32
Table 4.3: AAD between water and 0.5wt% ethanol data for bubble column and three-phase fluidized bed. Here the AAD is defined as $((\varepsilon_{\text{ethanol}} - \varepsilon_{\text{water}})/\varepsilon_{\text{water}})$	51
Table 4.4: Average absolute deviation (AAD) and bias factor (F_m) for the Han et al. (1990) correlation based on the experimental phase holdups in figures 4.10 and 4.13 ..	57
Table 4.5: Dimensionless groups used in Larachi et al. (2001) three-phase fluidized bed holdups correlations.....	58
Table 4.6: Average absolute deviation (AAD) and bias factor (F_m) for the Larachi et al. (2001) correlation based on the experimental phase holdups in figures 4.10 and 4.13.	59

List of figures

Figure 1.1: Schematic of a three-phase fluidized bed (Fan, 1989).....	1
Figure 1.2: Adsorption and concentration of surfactant at an interface. (Porter, 1994).....	4
Figure 1.3: Schematic description of surface tension gradient induced flow, i.e. Marangoni effect. (Schramm, 1994)	5
Figure 2.1: Schematic of the multiphase system. Valves in black are closed to flow.....	9
Figure 2.2: Schematic of maximum pressure bubble method for measuring dynamic surface tension.....	10
Figure 2.3: Dynamic pressure profile in an air, water and 5 mm diameter glass beads: $U_L = 0.07$ m/s and $U_g = 0.0516$ m/s.	17
Figure 2.4: Dynamic pressure profile in an air, 5% wt. ethanol solution and 5 mm diameter glass beads: $U_g = 0$ m/s.....	19
Figure 3.1: Coalescence percentage in aqueous solutions of aliphatic alcohols (Zahradnik et al., 1999).....	21
Figure 4.1: Equilibrium and dynamic surface tension of aqueous solutions.....	25
Figure 4.2: Foam heights versus superficial gas velocity for the alcohol solutions.....	27
Figure 4.3: Overall gas holdup versus U_g for all liquids in the bubble column at $U_L = 0$ and 0.07 m/s.....	29
Figure 4.4: Comparison of gas holdup data for water and 0.5% wt. ethanol solution at $U_L = 0$ and 0.07m/s.....	31
Figure 4.5: Comparison of experimental gas holdups to the predictions of the correlations of Hikita et al. (1980) and Luo et al. (1990) for tap water and 0.5% wt. ethanol solution.	34
Figure 4.6: Comparison of bubble column gas holdups at $U_L = 0$ for tap water with various literature data.	35
Figure 4.7: Comparison of bubble column gas holdups at $U_L = 0$ and 0.07 m/s for the 0.5% wt. ethanol solution with the data of Kelkar et al. (1983).	35
Figure 4.8: Comparison of experimental gas hold-ups to the prediction of the correlations of Hikita et al. (1980) and Luo et al. (1990) after adjusting the constant.	36
Figure 4.9: Fluidized bed phase holdups versus superficial gas velocity for all liquids at $U_L = 0.0187$ m/s with the 1.2-mm glass beads.....	38
Figure 4.10: Fluidized bed freeboard gas holdups versus superficial gas velocity for all liquids at $U_L = 0.0187$ m/s with the 1.2-mm glass beads.	39
Figure 4.11: Fluidized bed phase holdups versus superficial gas velocity with the 1.2-mm glass beads. Open and closed symbols are for $U_L = 0.0187$ and 0.067 m/s respectively. Diamond and triangle symbols are for tap water and 0.5% wt. ethanol solution respectively.	40
Figure 4.12: Fluidized bed and freeboard gas holdups with the 1.2-mm particles for both water and 0.5% wt. ethanol solution. Diamond and triangle symbols are for the bed and freeboard gas holdups, respectively. Open and closed symbols for $U_L = 0.0187$ and = 0.067 m/s, respectively.....	42
Figure 4.13: Fluidized bed phase holdups versus superficial gas velocity for all liquids at $U_L = 0.073$ m/s with the 5-mm glass beads.....	44

Figure 4.14: Fluidized bed phase holdups versus superficial gas velocity with the 5-mm glass beads. Open and closed symbols are for $U_L = 0.073$ and 0.173 m/s respectively. Diamond and triangle symbols are for tap water and 0.5% wt. ethanol solution respectively.	46
Figure 4.15: Fluidized bed and freeboard gas holdups with the 5-mm particles for both water and 0.5% wt. ethanol solution. Diamond and triangle symbols are for the bed and freeboard gas holdups, respectively. Open and closed symbols for $U_L = 0.73$ and $= 0.173$ m/s, respectively.	48
Figure 4.16: Comparison of freeboard gas holdup for particle size 1.2mm and 5mm with bubble column at $U_L=0.07$ m/s for both water and 0.5%wt ethanol solution....	49
Figure 4.17: Three-phase fluidized bed gas holdups for water and 1%wt ethanol solution and for particle sizes of 1.2-mm and 4-mm from the work of Nacef (1991). ..	52
Figure 4.18: Comparison of experimental fluidized bed gas holdups to the predictions of the correlation of Han et al. (1990) for tap water and 0.5% wt. ethanol solution with the 1.2-mm particles at $U_L = 0.0187$ and 0.0677 m/s.	55
Figure 4.19: Comparison of experimental fluidized bed gas holdups to the predictions of the correlation of Han et al. (1990) for tap water and 0.5% wt. ethanol solution with the 5-mm particles at $U_L = 0.073$ and 0.173 m/s.	56
Figure: 4.20 Minimum liquid fluidization velocity versus superficial gas velocity for several liquids and for the 1.2 and 5-mm glass beads.....	61
Figure 4.21: Minimum liquid fluidization velocity versus superficial gas velocity for several liquids and for the 1.2, 2 and 4-mm glass beads for various liquids from Nacef (1991).....	63

Acknowledgements

I would like to first express my sincere gratitude to Dr. Arturo Macchi for his guidance, support and inspiration during this work. He has done everything to make this project an enjoyable experience.

My appreciation also goes to all who work in the department.

I would like to sincerely thank my fellow classmates and friends who made my life in Ottawa entertaining. Finally, I would like to thank my family for loving and believing in me.

1. Introduction

Three-phase fluidized beds are employed in a wide range of applications that require intimate contact between a gas, a liquid and solid particles. Industrial applications are found in hydrocracking of heavy oil fractions, Fischer-Tropsch synthesis, aerobic wastewater treatment, production of pharmaceuticals via plant and animal cells, etc. (Fan, 1989). Although several configurations can exist for these multiphase contactors, this thesis will address the case where gas and liquid are flowing upwards through the fluidized bed of solid particles. The liquid is the continuous phase while the gas and solids are the dispersed phases. Figure 1.1 presents a schematic of such a three-phase fluidized bed.

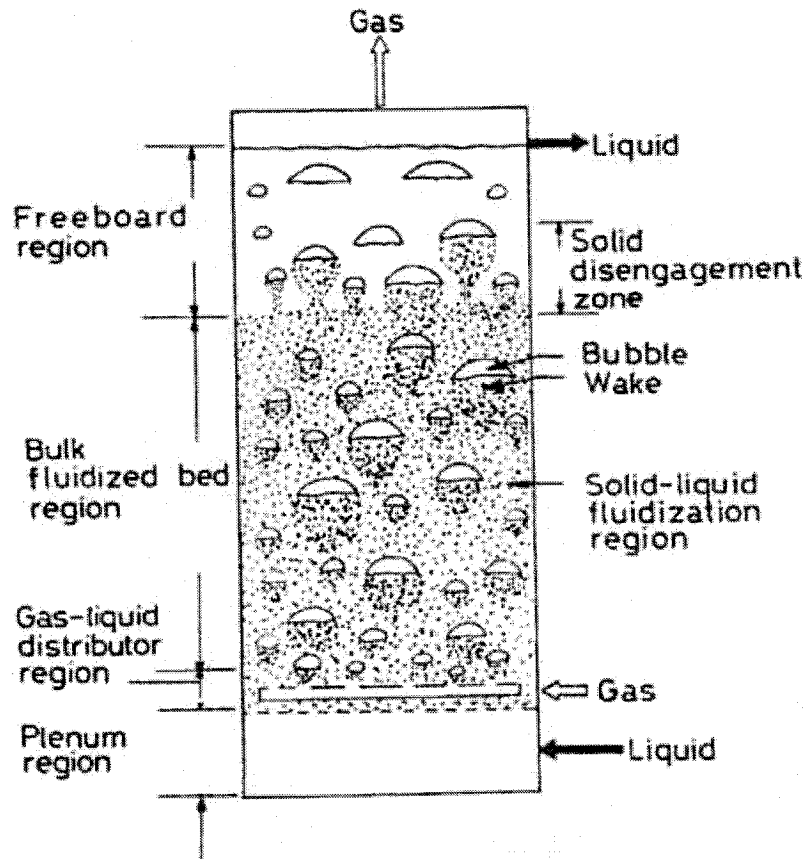


Figure 1.1: Schematic of a three-phase fluidized bed (Fan, 1989).

There are three distinct regions in a three-phase fluidized bed: the distributor, the bulk and the freeboard. The distributor region refers to the area immediately above the gas-liquid distributor where gas jets may occur. It is the region from initial bubble formation to the establishment of final bubble size. The bulk fluidized bed region includes the main portion of the bed. The freeboard is the gas-liquid region above the bed surface and may contain entrained particles from the bulk region. The demarcation between the freeboard and the bulk fluidized bed regions is more distinct for large/heavy particles than for small/light particles (Fan, 1989).

Hydrodynamic features of these multiphase contactors are a complex function of physical properties of the phases, operating conditions and reactor geometry. In general, the hydrodynamic behaviour of three-phase fluidized beds can be characterized by bubble properties (size and size distribution, shape and rise velocity) and phase holdups (phase volumetric fraction). These parameters, in turn, affect mass and heat transfer rates and mixing and flow patterns of the liquid and solids. Bubble dynamics also dictate the resulting flow regime. At low gas flowrates, small bubbles of uniform size are produced with little interaction between them. The flow regime is referred to as the “dispersed bubble flow regime”, and an increase of gas flowrate increases the bubble population more than the bubble size. However, this flow regime cannot be sustained indefinitely. Beyond a certain gas flowrate, the bubble population becomes sufficiently large that bubbles start to coalesce and travel faster than their smaller counterparts. There is now a wide bubble size distribution, which induces relatively strong liquid circulation patterns and mixing. This flow regime is referred to as the “coalesced bubble flow regime”.

There has been a significant amount of research on the hydrodynamics and heat and mass transfer properties of three-phase fluidized beds under ambient operating conditions using air, water and glass beads (Wild and Poncin, 1996). However, the physical properties of such systems differ considerably from those found in most industrial units which usually contain multi-component organic liquids and operate at greater pressures and temperatures. Furthermore, the physicochemical properties of the phases in commercial systems are not always well defined and may significantly change with the progress of the reactions.

1.1 Surfactants and their effects on bubble dynamics

The gas holdup is very sensitive to surface-active agents found in multi-component liquids. The addition of solutes (e.g. alcohols, proteins, organic acids, electrolytes, surfactants) and/or finely divided particulates (e.g. catalyst, clays, emulsions) to a liquid can enhance but usually severely hinder bubble coalescence.

Surfactants are composed of two parts: a long tail which is hydrophobic and a bulged circular structure that is hydrophilic. They thus tend to accumulate at the gas-liquid interface and lower interfacial tension by providing an expansion force acting against the normal interfacial tension (Schramm, 1994). As there is a balance between adsorption and desorption due to thermal motions, the interfacial condition requires some time to establish. Thus, surface activity should be considered a dynamic phenomenon.

From figure 1.2, at very low surfactant concentration there is no orientation and the molecules lie flat on the surface. As the concentration increases, the number of surfactant molecules on the surface increases and there is not sufficient room to lie flat on the surface. They thus begin to orient and the orientation depends on the nature of the hydrophilic group and the surface. At a certain concentration called the critical micelle concentration (CMC), the number of surfactant molecules available is now sufficient to form a unimolecular layer at the interface. The surfactant molecules in the bulk solution will then form an ordered structure known as a micelle so long as the concentration is above the CMC. The CMC indicates the point at which monolayer adsorption is complete and there is no change in surface tension with increasing surfactant concentration.

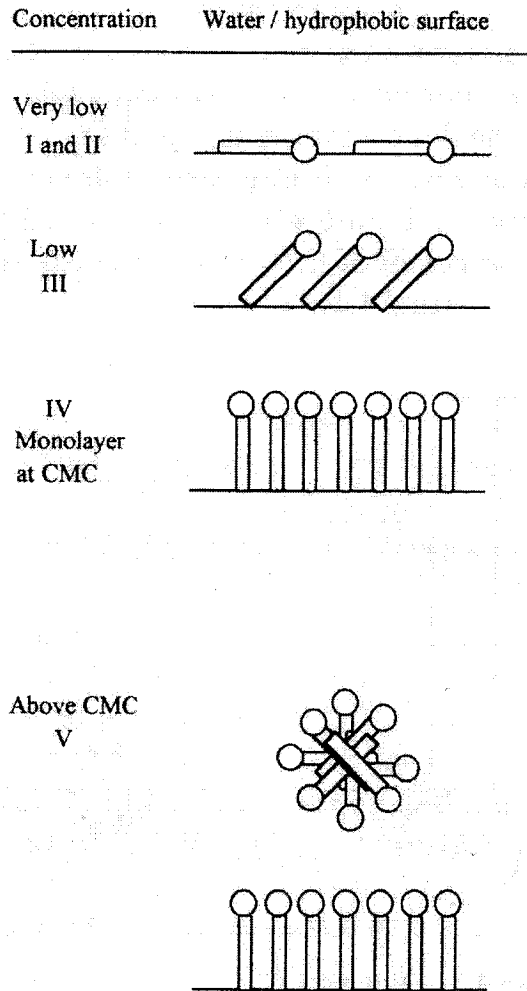


Figure 1.2: Adsorption and concentration of surfactant at an interface. (Porter, 1994)

Surfactants affect bubble dynamics in three ways. First, the average bubble size is generally reduced due to a reduction in surface tension. This leads to an increase in the bubble interfacial area and a decrease in its rise velocity. Second, surface tension gradients are developed around the bubble surface immobilizing it (i.e. reducing the internal gas circulation rate), which leads to an increase in drag and thus a reduction in the bubble rise velocity. Finally, the coalescence of bubbles is inhibited as will be described shortly below. All three effects tend to keep the average bubble size small and rise velocity low. This in turn affects the gas holdup, phase mixing and interphase mass transfer. In dispersed bubble flow, the bubble rise velocity (U_b), gas holdup (ϵ_g) and superficial gas velocity (U_g) are interrelated as shown in equation 1.1. The bubble rise velocity is proportional to the bubble diameter.

$$\varepsilon_g = \frac{U_g}{U_b} \quad (1.1)$$

Coalescence of two gas bubbles in a liquid occurs in three steps. First, bubbles approach each other trapping a small amount of liquid between them. Next, this liquid drains until the film separating the bubbles reaches a critical thickness. Finally, at this critical point, the film ruptures resulting in bubble coalescence. The rate-limiting step is usually the liquid film drainage. If a surfactant-stabilized film undergoes sudden expansion due to liquid drainage, then the expanded portion of the film has a lower concentration of surfactant because of the greater surface area (see figure 1.3). This causes an increased local surface tension that provides increased resistance to further expansion. A local rise in surface tension produces immediate contraction of the surface and coupled with viscous forces, induces liquid flow in the thin film from the low to the high surface tension region. The transport of bulk liquid due to surface tension gradients is termed the Marangoni effect and provides resistance to film thinning by gravity and capillary pressure (Schramm, 1994; Garrett 1993).

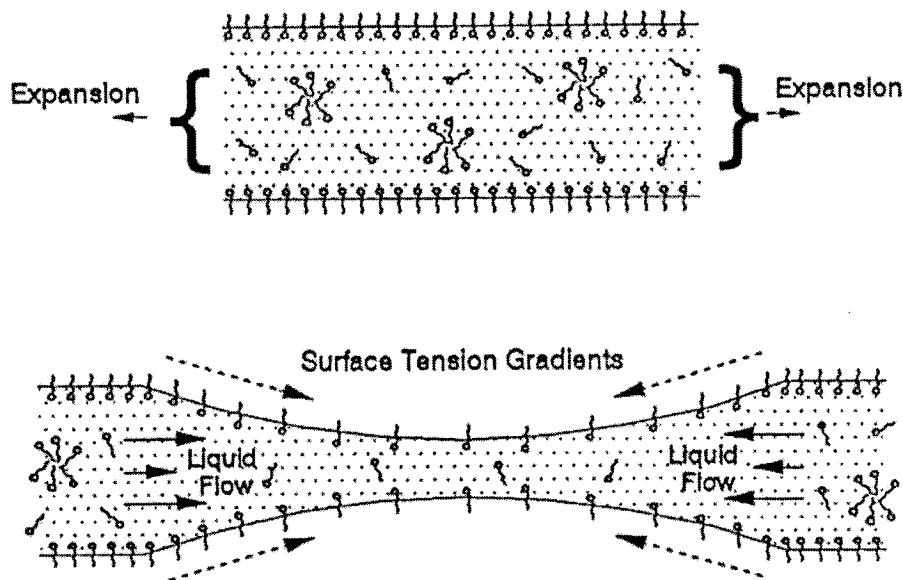


Figure 1.3: Schematic description of surface tension gradient induced flow, i.e. Marangoni effect. (Schramm, 1994)

1.2 Approaches to model phase holdups in the presence of surfactants

Unfortunately no applicable equations describing the relationship between the physical properties of a multi-component liquid and the degree of bubble coalescence are available to predict the hydrodynamic features of multiphase reactors (Chaudhari and Hofmann, 1994; Zahradnik et al., 1999; Larachi et al., 2001). Most hydrodynamic models and correlations assume that the major physical properties of the liquid (i.e. density, viscosity, equilibrium surface tension) are sufficient to characterize bubble dynamics (Fan, 1989; Wild and Poncin, 1996). While this is true for pure liquids (Wilkinson et al., 1992), multi-component liquids will often require additional properties due to interfacial phenomena. For example, Saberian-Broudjenni et al., (1987) performed a systematic study on the effect of liquid properties in three-phase fluidized beds using cyclohexane, kerosene, gas oil, CCl₄ and water. They compared kerosene to cyclohexane (both liquids having very similar physical properties) and observed completely different fluidizing behaviour due to the foaming nature of kerosene. Cyclohexane being a monocomponent liquid does not foam. Bed expansions and gas holdups in the kerosene system were consistently greater than those for cyclohexane at similar operating conditions.

Attempts have been made to incorporate the effects of surfactants on bubble coalescence and break-up, but these correlations and models are usually only suitable for binary solutions with a specific surfactant (e.g. alcohol, salt) and/or require a priori knowledge of physical characteristics that are not easily estimated such as the bubble diameter, the Hamaker-London constant or foam height (Kelkar et al., 1983; Keitel and Onken, 1982; Koide et al., 1985; Chaudhari and Hofmann, 1994; Sultana et al., 2002). As mentioned, in many practical cases it is impossible to identify all solutes present in the multi-component liquid. To date, the mostly widely used equations to estimate phase holdups in three-phase fluidized beds are the empirical correlations developed by Han et al (1990) and Larachi et al. (2001) since they have incorporated a very large amount of data from several sources using pure (mainly) and multi-component liquids.

Finally, Gorowara and Fan (1990) presented an interesting approach to determine the gas holdups of a three-phase fluidized bed without the need to know the concentration or type(s) of surface-active agents present in the solvent. They first measured the dynamic surface tension of their surfactant solutions, they then grouped the liquids based on the dynamic behaviour of the surface tension, and they finally proposed gas holdup correlations for each liquid group.

1.3 Thesis objectives and outline

The following goals provide the scope for the present work:

1. Evaluate the effect of surface-active agents on the hydrodynamics (phase holdups and minimum liquid fluidization velocity) of a gas-liquid bubble column and gas-liquid-solid fluidized bed. There are very few systematic studies on the effects of surfactants in both two- and three-phase systems and should help elucidate the role of particles on the effects of surfactants.
2. Compare and relate the gas holdups in the bed and freeboard of a three-phase fluidized bed.
3. Test the phase holdup prediction approach proposed by Gorowara and Fan (1990).

The thesis outline is as follows: The experimental system and measurement techniques are presented in Chapter 2. Chapter 3 describes the strategies employed to select the surface-active agents as well as the operating conditions. Chapter 4 presents the results and discussions. Finally, the thesis presents conclusions and options for future research in Chapter 5.

2. Experimental system and measurement techniques

The following section presents the multiphase fluidization system employed as well as the measurement techniques used to characterize the liquid physical properties and to measure the relevant hydrodynamic features.

2.1 Multiphase fluidization system

Figure 2.1 is a schematic of the multiphase fluidization system. The column is made of acrylic with an inner diameter of 0.15 m and a height of 2.75 m, and is equipped with a large number of ports so that the necessary instruments (e.g. pressure transducers, dissolved oxygen probe, heat transfer probe) for hydrodynamic characterization can be installed at different heights and radial positions. Data logging equipment and software (Labview 7.0) are used to facilitate data acquisition.

When the system operates as a gas-liquid-solid fluidized bed, a centrifugal pump drives the liquid from the storage tank to the column base. Globe valves and a by-pass loop control the liquid flow. Pressurized air is fed to the column base once the pressure and flow are adjusted with a pressure regulator and needle valve. The gas and liquid are introduced into the bed of particles separately, but at the same level. This allows individual distributor designs for uniform (or selected non-uniform) spatial distribution of the fluids. The liquid distributor is a perforated plate with 80 holes of 3.97 mm diameter, while the gas is introduced via 86 holes of 0.794 mm diameter. At the top of the column, a simple overflow system is used as a first stage of gas-liquid separation. The gas is vented to the atmosphere, while the liquid is directed to the partitioned storage tank for further degassing. Rotameters monitor the liquid and gas flow rates. The multiphase system can also operate as gas-liquid bubble column with the gas passed from the bottom of the column and with the liquid being batch or circulating co-currently with the gas.

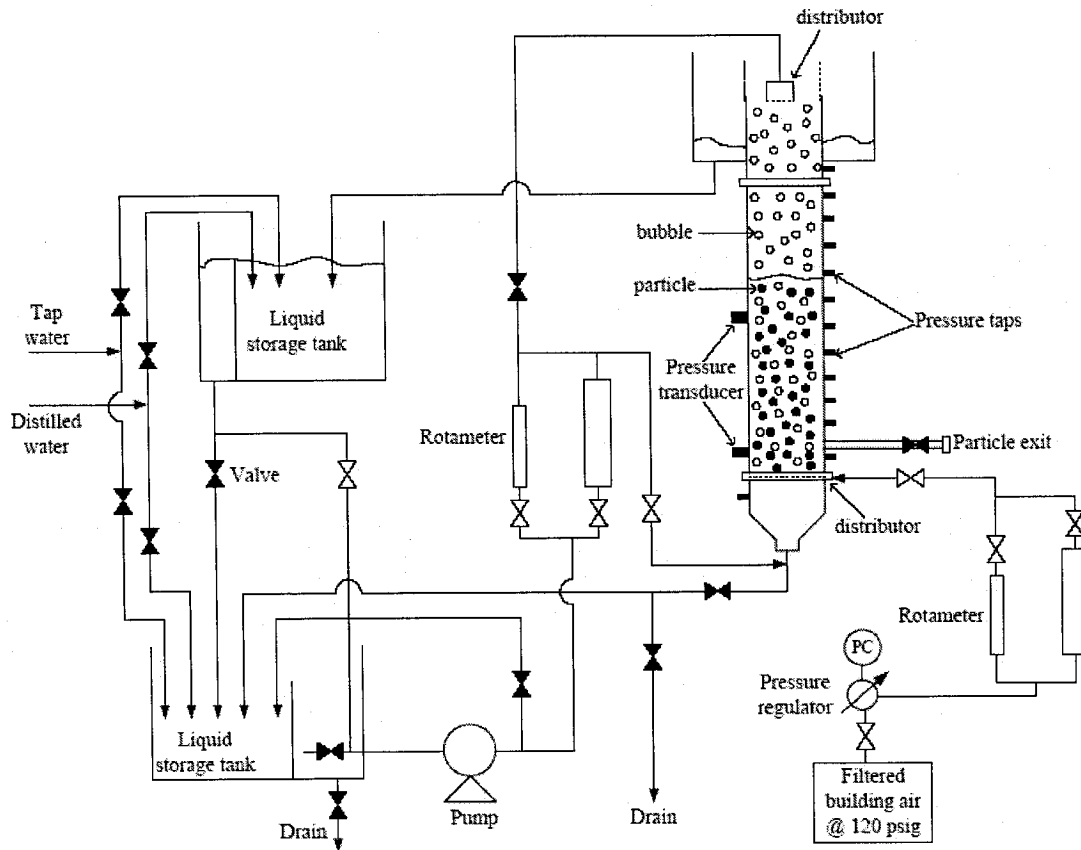


Figure 2.1: Schematic of the multiphase system. Valves in black are closed to flow.

2.2 Liquid phase characterization

The physical properties investigated are the surface tension and foaming characteristics of the surface-active solutions.

2.2.1 Surface tension

The equilibrium surface tension of the liquid was measured by the Wilhelmy plate method using a Kruss K12 tensiometer. A thin plate with a perimeter of 40 mm is lowered to the surface of the liquid and the downward force directed to the plate is measured. Surface tension is obtained by dividing the force by the perimeter of the plate.

The dynamic surface tension was obtained using the Sensodyne QC6000 Version 1.4.1, which is based on the maximum pressure bubble method. This technique measures the maximum pressure necessary to blow a bubble in a liquid from the tip of a capillary (0.5 mm

in diameter). In practice, the pressure increases within the capillary at constant gas flowrate until a bubble appears at the tip of the orifice. The Young-Laplace equation (Eq. 2.1) relates the pressures inside and outside the bubble to the capillary orifice radius and liquid surface tension.

$$\Delta P = 2\sigma/r \quad (2.1)$$

A schematic of the apparatus is shown in figure 2.2. The larger capillary (4 mm in diameter) is a reference, eliminating hydrostatic pressure. This technique yields the dynamic surface tension for a specific bubbling rate.

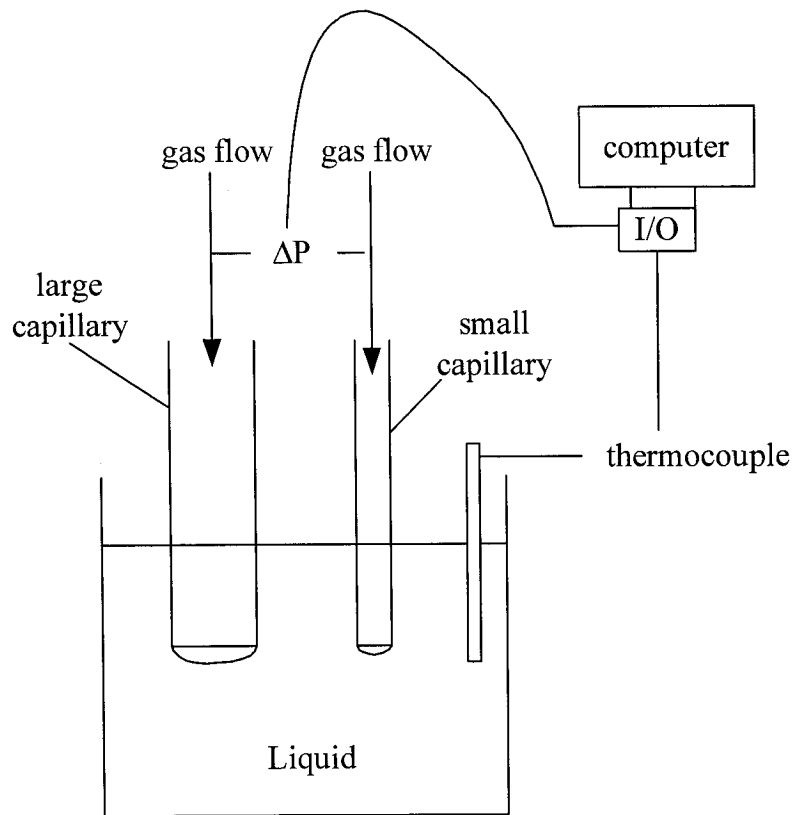


Figure 2.2: Schematic of maximum pressure bubble method for measuring dynamic surface tension.

The flow of gas (nitrogen in this case) to the probes is controlled with mass flow controllers allowing bubbles to be formed at different frequencies and thus to detect the dynamic nature

of the liquid surface tension. The value of surface tension measured in this process is governed by the rate of diffusion of the surfactant molecules from the bulk towards the growing gas bubble.

The surface tensiometer was calibrated over the range of desired values using deionized water and ethanol at room temperature. Furthermore, the tensiometer is required to be recalibrated for every new set of operating conditions (change in bubble frequency and/or temperature), and this was executed for each different case in the present experiments. Four to five data points are obtained for a single bubble frequency and surface tension values varied within 0.1 mN/m.

2.2.2 Dilatational elasticity

The dissipation of surface tension gradients to achieve equilibrium effectively provides the interface with a finite elasticity. Surface elasticity can be measured directly or obtained by measurements of dynamic surface tension coupled with some information about surfactant diffusion rates (Schramm, 1994). Therefore, the maximum pressure bubble method can also be used to determine the surface elasticity. The dilatational surface elasticity (E_M) is defined as the surface tension variation with respect to the bubble surface unit fraction area (A_b) change, i.e.

$$E_M = d\sigma/d \ln A_b = A_b d\sigma/dA_b \quad (2.2)$$

Here A_b can be characterized by the tip diameter of the small capillary, thus dA_b/A_b is proportional to the rate of bubble formation since approximately equal bubble areas are produced at the maximum bubble pressure condition for all bubbling rates (Huang et al., 1986). The dilatational surface elasticity is then directly proportional to the slope of the dynamic surface tension as a function of the bubbling rate. Huang et al. (1986) also evaluated the dilatational surface elasticity of alpha-olefin sulfonates in aqueous solutions. Their results suggested that a greater surface elasticity leads to more stable bubbles resulting in greater foam retention and half-life times, which are defined in the following section.

2.2.3 Foam retention and half-life times

Foaming occurs when relatively small gas bubbles are injected at a rate such that the rate of liquid film drainage is slow enough that the bubbles form clusters. Once foam is formed, the foam height reaches a state of equilibrium where the rates of formation and decay balance each other. The bubble column was used to evaluate the foam-forming tendency of the liquids. Air was gently bubbled into the stagnant body of liquid and the foam head was monitored. Two foaming parameters can be derived from this exercise (Bickerman, 1973):

1. Foam retention time (R_f), which is the ratio of the foam volume generated at a given gas flowrate to that flowrate.

$$R_f = \frac{\text{foam volume}}{\text{gas flowrate}} \quad (2.3)$$

2. Foam half-life ($t_{f,(1/2)}$) is determined from the collapse curve once the gas flow has been stopped. Assuming that first-order kinetics describe the foam volume decay:

$$t_{f,(1/2)} = \frac{0.693}{k_f}, \quad \text{where } k_f \text{ is the foam decay rate constant} \quad (2.4)$$

2.2.4 Liquid categorization proposed by Gorowara and Fan (1990)

Gorowara and Fan (1990) presented an interesting approach to determine the gas holdups in three-phase fluidized beds based on the measurement of the liquid dynamic surface tension. They first proceeded to define three parameters:

- (1) The surface pressure Π_s which is the surface tension drop caused by the surfactant,

$$\Pi_s = \sigma_w - \sigma_e \quad (2.5)$$

where σ_w is the surface tension of solvent and σ_e is the equilibrium surface tension measured by the Wilhelmy Plate method.

(2) Difference between the dynamic and equilibrium surface tension, σ_m .

$$\sigma_m = \sigma_e - \sigma_b(0.5) \quad (2.6)$$

where $\sigma_b(0.5)$ is the dynamic surface tension measured using the maximum pressure bubble method at an arbitrary bubbling rate of 0.5 bubbles/s.

They suggested that large values of this parameter (> 1 mN/m) are probably due to impurities in the surfactant itself. The impurity may not be evenly dispersed throughout the solution, but preferentially adsorbed at the static gas-liquid interface above the capillary orifice. The impurity would then not adsorb fast enough to a newly formed interface (bubble surface) in the bulk of the solution. This would lead to equilibrium surface tensions lower than that measured by the maximum pressure bubble method. Alternatively, these values may also differ when the surfactant is pure and well dispersed in the liquid bulk but its diffusion to the interface is mass transfer limited at a bubble rate of 0.5 bubbles per second, see parameter 3. A faster or slower bubbling rate could potentially change this parameter.

(3) Average variation of surface tension with bubble rate, $\Delta\sigma_b/\Delta br$. This parameter is proportional to the dilatational surface elasticity of the bubble, see section 2.2.2.

$$\frac{\Delta\sigma_b}{\Delta br} = \frac{\sigma_b(4.0) - \sigma_b(0.5)}{4.0 - 0.5} \quad (2.7)$$

The limited range of bubbling rate was due to the capacity of the experimental apparatus used at the time. Moreover, it would have been preferable that the surface tension be measured for a specific bubble surface age. The bubble surface age does not scale linearly with the inverse of the bubbling rate and it is the former that is important in determining the surface tension.

Gorowara and Fan (1990) then combined these three parameters into four categories of liquids which show different hydrodynamic characteristics.

- Liquid category 1

In this category liquids are water-like with Π_s and σ_m less than 1 mN/m, and $\Delta\sigma_b/\Delta br$ less than 1 (mN/m)/s.

- Liquid category 2

Category 2 contains solutions with Π_s greater than 1 mN/m, but σ_m and $\Delta\sigma_b/\Delta br$ less than 1 mN/m and 1 (mN/m)/s respectively.

Surfactants in this category are well dispersed throughout the liquid solution and quickly diffuse to the newly formed bubble surface.

- Liquid category 3

In this category, both Π_s and σ_m are greater than 1 mN/m, but $\Delta\sigma_b/\Delta br$ is less than 1 (mN/m)/s.

Such liquids support the theory that some surfactants have impurities (e.g. oils) that are not well dispersed in the bulk solution. However, the selected surfactant itself is well dispersed in the bulk solution and quickly adsorbs onto the fresh bubble surface. Gorowara and Fan (1990) found that most commercial surfactants belong to this category.

- Liquid category 4

Category four contains solutions in which the parameters Π_s and $\Delta\sigma_b/\Delta br$ are greater than 1 mN/m and 1 (mN/m)/s respectively. Large values of $\Delta\sigma_b/\Delta br$ suggests that the diffusion of

surfactant molecules from the bulk solution to the bubble surface and their subsequent adsorption are rate limiting.

Gorowara and Fan (1990) finally proceeded to correlate the gas holdups in a three-phase fluidized for each category of liquid. Liquids that present relatively low gas holdups belong to categories 1 and 4, those with medium gas holdups to category 3 and potentially category 2 if $\Pi_s < 2$ mN/m, and those with relatively high gas holdups to category 2 if $\Pi_s > 2$ mN/m.

- Liquids that present low gas holdups (categories 1 and 4)

$$\varepsilon_g = 0.132 Fr_g^{0.2855} Re_L^{-0.0892} \quad (2.8)$$

- Liquids that present moderate gas holdups (category 3, and category 2 if $\Pi_s < 2$ mN/m)

$$\varepsilon_g = 0.132 Fr_g^{0.3117} Re_L^{0.1166} \quad (2.9)$$

- Liquids that present high gas holdups (category 2 if $\Pi_s > 2$ mN/m)

$$\varepsilon_g = 0.8140 Fr_g^{0.3987} Re_L^{-0.0977} \quad (2.10)$$

The approach and gas holdup correlations were developed with a system composed of air, various aqueous solutions and spherical glass beads of 1.5 mm in diameter and 2500 kg/m³ in density. The gas superficial velocity varied between 0.007 and 0.07 m/s while the liquid superficial velocity ranged from 0.018 to 0.067 m/s. The column had an inner diameter of 0.102 m and the static bed height was 0.25 m. It is interesting to note that the dependency of gas holdup on liquid velocity (Re_L) for the medium gas holdup correlation (Eq. 2.9) is opposite to that for the low and high gas holdup correlations (Eqs. 2.8 and 2.10).

The manner in which they grouped their liquids is interesting. As expected, liquids in category 1 present characteristics of pure liquids or solutions with an insufficient

concentration of surfactant and thus should present low gas holdups. Category 2 liquids show the greatest gas holdups if the surfactant concentration is sufficiently high. The reasoning is that the surfactant molecules are plentiful and are quickly adsorbed onto the bubble surface where they can be active in reducing the surface tension and the internal circulation rate of gas. Category 3 liquids present middle gas holdups although it is not obvious why they should be any different than those of category 2 since the surfactant of interest is well dispersed and quickly adsorbs onto the bubble surface. Finally category 4 liquids are grouped with the water-like liquids which present relatively low gas holdups. Gorowara and Fan (1990) reasoned that the surfactant molecules did not have the time to migrate to the bubble surface and be active. This may be true in dispersed bubble flow where bubbles do not interact and the role of adsorbed surfactant molecules is mainly to reduce the surface tension and immobilize the surface. However for foaming to occur, there must be significant bubble coalescence inhibition due to the Marangoni effect (see section 1.1.) and thus significant values of $\Delta\sigma_b/\Delta br$. Therefore it is strange that liquids in category 4 present low gas holdups. Perhaps, the entire approach holds in dispersed bubble flow (far from the natural transition) where the surfactants do not inhibit bubble coalescence but reduce the bubble size and rise velocity.

2.3 Hydrodynamic parameters

The relevant hydrodynamic parameters measured are the phase holdups and the minimum liquid fluidization velocity.

2.3.1 Phase holdups

Overall holdups in all multiphase systems were obtained by measuring the dynamic pressure drop along the column at several levels. A differential pressure transducer, PX750-30DI from Omega, was used. The pressure reading accuracy was 0.25% of the calibrated scale. The reference port was situated 57 mm above the distributor. At each position, the pressure difference was recorded for 120 s periods at 100 Hz. Figure 2.3 presents a typical pressure profile. The dynamic pressure drop ($-\Delta P$) is defined as the total pressure gradient corrected for the hydrostatic head of liquid (i.e. $-\Delta P = -\Delta P_T - g\rho_L\Delta z$).

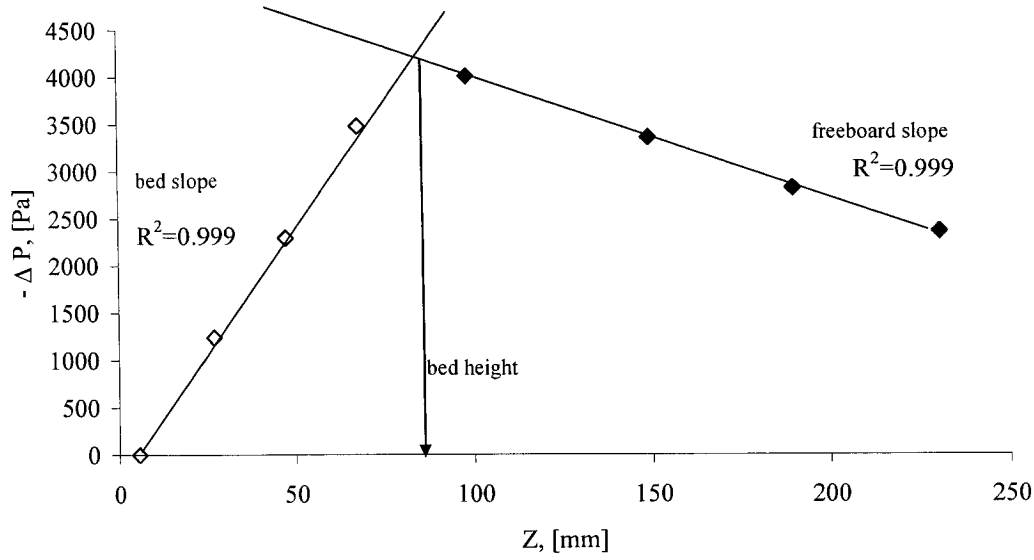


Figure 2.3: Dynamic pressure profile in an air, water and 5 mm diameter glass beads: $U_L = 0.07$ m/s and $U_g = 0.0516$ m/s.

The bed height and hence bed expansion are determined from the intersection of the bed and freeboard pressure drop lines obtained by linear regression. The solids holdup (ϵ_s) can then be obtained from:

$$\epsilon_s = \frac{4M}{\pi D^2 H_b \rho_p} \quad (2.11)$$

Where M is the weight of particles contained in the bed, ρ_p is the particle density and H_b is the bed height. The bed expansion is related to the solids holdup by:

$$\text{Bed expansion (\%)} = 100 \left(\frac{\epsilon_{smf}}{\epsilon_s} - 1 \right) \quad (2.12)$$

where ϵ_{smf} is the solids holdup at minimum fluidization. Neglecting the frictional drag on the wall and accelerations of the phases in the vertical direction, the gas holdup (ϵ_g) is related to the dynamic pressure drop by:

$$\varepsilon_g = \frac{(\varepsilon_s(\rho_p - \rho_L) + \Delta P / g\Delta z)}{(\rho_L - \rho_g)} \quad (2.13)$$

The slopes of the pressure drop lines are used to calculate the gas holdups. In figure 2.3, the regressions are linear ($R^2 \approx 1$). Assuming that ε_s is independent of z , axial variation of gas and liquid holdups can be considered negligible. From visual observation, for all experiments presented in this thesis, only negligible volumes of particles were entrained in the freeboard.

Finally, since the sum of the phase volume fractions must be unity, the liquid holdup is:

$$\varepsilon_L = 1 - \varepsilon_g - \varepsilon_s \quad (2.14)$$

2.3.2 Minimum liquid fluidization velocity

Minimum liquid fluidization velocity (U_{Lmf}) is the lowest liquid velocity which brings the particles from rest to motion at any fixed gas velocity. For a given gas velocity, the minimum liquid fluidization velocity could be estimated using the plot of pressure gradient versus the superficial liquid velocity as shown in figure 2.4. The pressure drop over a certain length in the fixed bed follows the Ergun equation while the pressure drop over a certain length in the fluidized bed decreases with an increase in liquid flow rate due to a decrease in solids concentration.

Determination of U_{Lmf} for beds of small particle is more difficult than for beds of large particles and somewhat subjective since the transition from a fluidized to fixed bed is not distinct and abrupt. For small particles another hydrodynamic state (rather than fixed and fluidized) called heterogeneous is defined as the transition (Fan, 1989). The heterogeneous fluidization state is characterized by two zones with one consisting of a relatively dense fixed bed at the bottom and the other consisting of a fluidized bed at the top. Thus, it is hard to distinguish when the bed is completely fixed. Due to this difficulty, U_{Lmf} is usually predicted visually by researchers.

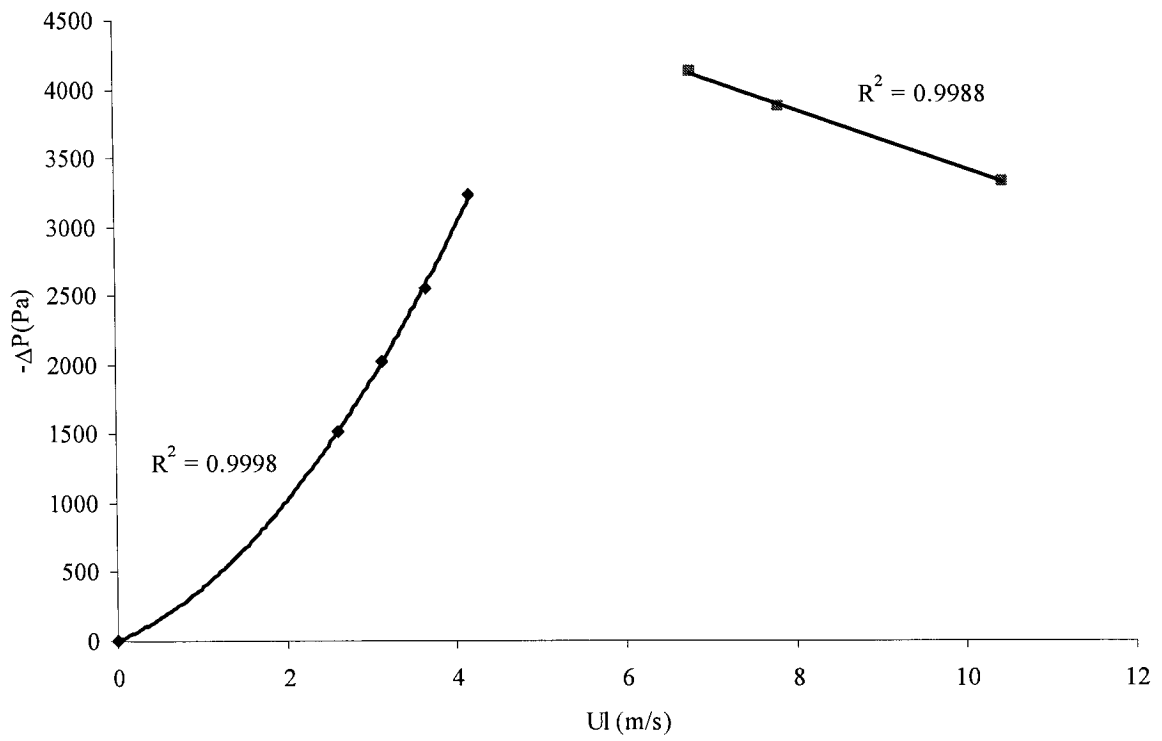


Figure 2.4: Dynamic pressure profile in an air, 5% wt. ethanol solution and 5 mm diameter glass beads: $U_g = 0$ m/s.

3. Selection of surface-active agents and operating conditions

The following section presents the strategies employed to select the types of surfactants as well as the operating conditions required to fulfill the research objectives.

3.1. Selection of surface-active agents in aqueous solutions

The solvent for all selected solutions is tap water. The first surface-active agent chosen was n-ethanol in concentrations below (0.5% wt.) and above (5% wt.) the critical transition concentration, c_t , which is defined as the concentration of solute where the probability of two bubbles injected towards each other to coalesce is 50% (Lessard and Zieminski, 1971). This parameter has been used to characterize the gas holdup in bubble columns (Zahradnik et al., 1999). Moreover ethanol solutions have been widely employed in bubble columns (Kelkar et al. 1983; Shah et al. 1985; Krishna et al. 2000) and less so in three-phase fluidized beds (Nacef, 1991). The coalescence probability as a function of the concentration of aqueous solutions of alcohols is presented in figure 3.1. The larger the molecular weight of the alcohol, the more surface-active it is and the lower the value of c_t .

The second surface-active agent chosen was n-pentanol in order to evaluate the effect of molecular weight as well as it has been employed in three-phase fluidized beds (Nacef 1991; Gorowara and Fan 1990). The solution concentration was chosen to be above c_t .

Three commercial surfactants (sodium dodecyl sulfate (SDS), hexadecyltrimethylammonium bromide (HTAB) and Triton X-100 which is an octylphenol ethoxylate) were then chosen since they respectively belong to anionic, cationic and non-ionic families and that they have similar molecular weights. In addition, for comparison purposes, there was dynamic surface tension data available in the literature for each surfactant. The surfactant concentration was kept below the CMC. Finally, but not least, the surface-active agents were selected to match the surfactant classification proposed by Gorowara and Fan (1990), which was presented in section 2.2.4.

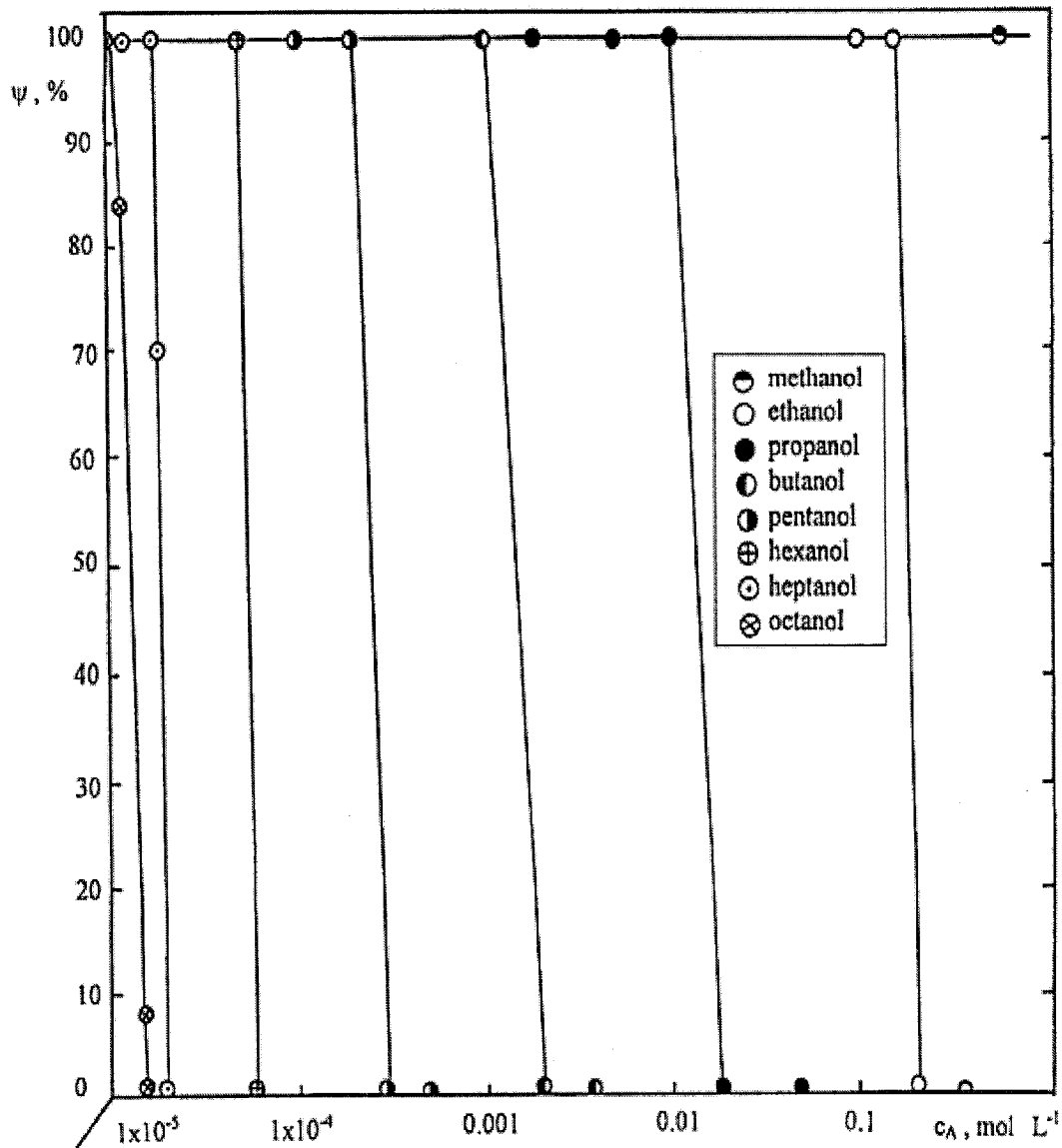


Figure 3.1: Coalescence percentage in aqueous solutions of aliphatic alcohols (Zahradnik et al., 1999).

Since the concentrations of the surface-active agents are relatively low, the liquid viscosities were approximated to that of water. The densities of the liquids were also approximated to that of water except for the 5% wt. ethanol solution which has a density of 989 kg/m³. This selection of surface-active agents thus allows isolating the effects of liquid surface tension on the hydrodynamic properties of the multiphase systems. Table 3.1 summarizes the chosen surface-active agents. The values of c_t were taken from Zahradnik et al. (1999)

while the CMC values of HTAB, and Triton X-100 and SDS were taken from Tomasic et al., (1999) and Manglik et al., (2001), respectively.

Table 3.1: Selection of surface-active agents.

Solute	Type	M.W. (g/mol)	C.M.C. (% wt.)	Ct (% wt.)	Concentration (% wt.)
n-ethanol	alcohol	46.07		0.81	0.5
n-ethanol	alcohol	46.07		0.81	5
n-pentanol	alcohol	88.15		0.0022	0.5
HTAB	cationic surfactant	364.45	0.033		0.01
Triton X-100	non-ionic surfactant	629	0.02		0.01
SDS	anionic surfactant	288.38	0.25		0.01

3.2. Selection of operating conditions

For each liquid, experiments were first conducted in a bubble column with no net liquid flow and then at a liquid superficial velocity of 0.07 m/s. Air was used as the gas and its superficial velocity was varied from 0.017 to 0.31 m/s in order to span the dispersed and coalesced bubble flow regimes.

Experiments were then conducted in the three-phase fluidized bed. Non-porous, spherical glass beads of 1.2 and 5 mm in diameter were used as particles. The particle density is 2500 kg/m³. The particles were chosen such that the liquid-solid fluidized bed would contract (with the smaller particles) and expand (with the larger particles) at the introduction of gas. This will allow investigating the effects of surfactants in two different types of gas-liquid-solid systems. The liquid superficial velocities were chosen such the two systems would operate at the same solids holdups (values of 0.27 and 0.52) before the introduction of the gas. Thus, the liquid superficial velocities were 0.0187 and 0.067 m/s, and 0.073 and 0.173 for the small and large particles respectively. The superficial gas velocity ranged from

0.0107 to 0.17 m/s in order to span the dispersed and coalesced bubble flow regimes. Finally, the common superficial liquid velocity of ~ 0.07 m/s was used to compare the gas holdups in the freeboard of the two different gas-liquid-solid systems with that of the circulating bubble column.

It is very important to note that the first liquid employed was the benchmark, tap water. After each aqueous solution had gone through all the different multiphase experiments, the system was thoroughly rinsed and filled with water. The bubble column gas holdups were then measured at selected gas velocities spanning dispersed and coalesced bubble flow in order to determine if trace amounts of remaining surfactant presented sufficient activity. In no case did the measured gas holdups differ more than 2% from the original measurements.

4. Results and discussions

The following section presents the experimental results and discussions concerning the characterization of the liquid physical properties as well as the hydrodynamic features of the bubble column and three-phase fluidized bed.

4.1 Characterization of liquid physical properties

As previously mentioned since the concentrations of the surface-active agents in the aqueous solutions are relatively low, the viscosities were approximated to that of water. The densities of the liquid solutions were also approximated to that of water except for the 5% wt. ethanol solution which gave a density of 989 kg/m³.

4.1.1 Surface tension

Figure 4.1 presents the surface tensions of the liquids solutions at different bubbling frequencies. The equilibrium surface tension, measured by the Wilhemy plate method, is the data point at the zero bubbling frequency. As expected the surface tension of tap water did not vary with bubbling frequency. The addition of ethanol to water decreases the equilibrium surface tension with the effect being greater for the more concentrated solution. The surface tension of the ethanol solutions only slightly increase with an increase in bubbling frequency as ethanol molecules can relatively quickly reach the bubble interface. In theory, at the limit of infinite bubble frequency, the surface tension of the liquid solution should reach that of the solvent, water. The drop in equilibrium surface tension and the effect of bubbling frequency on surface tension is more pronounced for the n-pentanol than for the n-ethanol solutions due the larger molecular weight of the solute. Finally, the surfactant solutions, which can be relatively grouped together, show the greatest surface activity as expected.

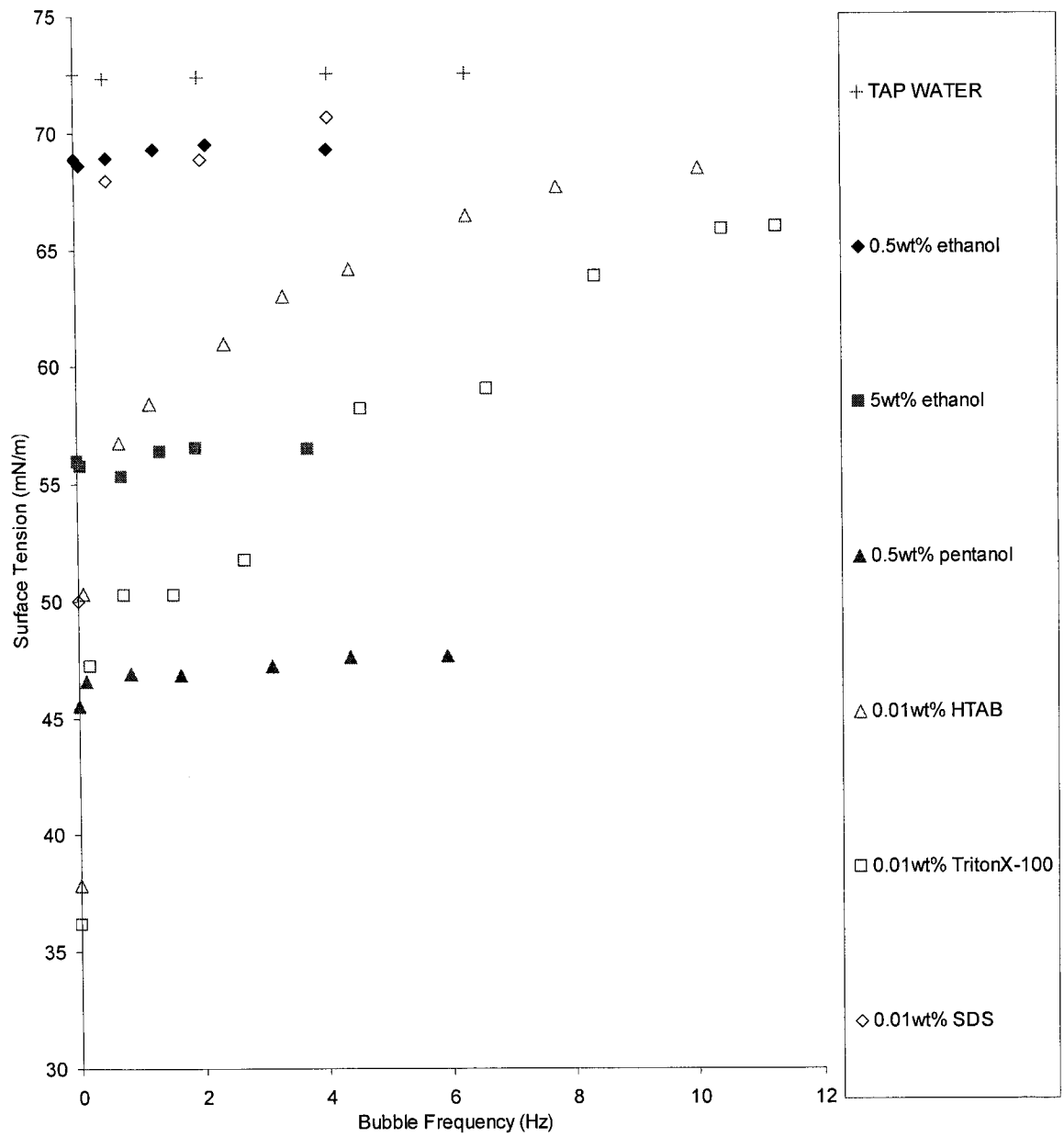


Figure 4.1: Equilibrium and dynamic surface tension of aqueous solutions.

From the dynamic surface tension data, the liquids were categorized according to the procedure proposed by Gorowara and Fan (1990). The results are summarized in table 4.1. The ethanol solutions fall in category 2, the pentanol and SDS solutions fall in category 3, and the HTAB and Triton X-100 solutions fall in category 4. These results should thus provide a good basis to test the gas holdup modeling approach proposed by Gorowara and Fan (1990).

Table 4.1: Analysis of surface tension data according to Gorowara and Fan (1990)

Solution	π_s	σ_m	$\Delta\sigma/\Delta br$	Category
Tap water	0	-0.14	-0.04	1
0.5% wt. ethanol	3.15	0.45	0.07	2
5% wt. ethanol	16.01	0.38	0.05	2
0.5% wt. pentanol	26.47	1.35	0.19	3
0.01% wt. HTAB	34.14	18.90	1.99	4
0.01% wt. Triton X-100	35.82	14.05	2.07	4
0.01% wt. SDS	21.99	17.95	0.77	3

4.1.2 Foam retention and half-life times

The measurement of the foam retention times was not possible for the surfactant solutions as the foam head overflowed the top of the column. Figure 4.2 thus presents the results obtained for the alcohol solutions only. The first observation is that the foam retention time is not constant as described in equation 2.3 but increases with increasing gas flow rate. Similar results were obtained by Czarnecki et al. (1982) who proceeded to measure the slope at the higher gas velocities. Secondly, it can be seen that the foam retention times increase with increasing solute concentration and molecular weight, with the latter having the greatest effect. It is interesting to note the foam retention times correlate with $\Delta\sigma_b/\Delta br$. As previously mentioned this parameter is proportional to the dilatational elasticity of the liquid and is an indication of foaming ability.

The half-life times of the foaming alcohol solutions were always less than a few seconds and were thus not possible to visually record. Half-life time tests were not performed on the surfactant solutions.

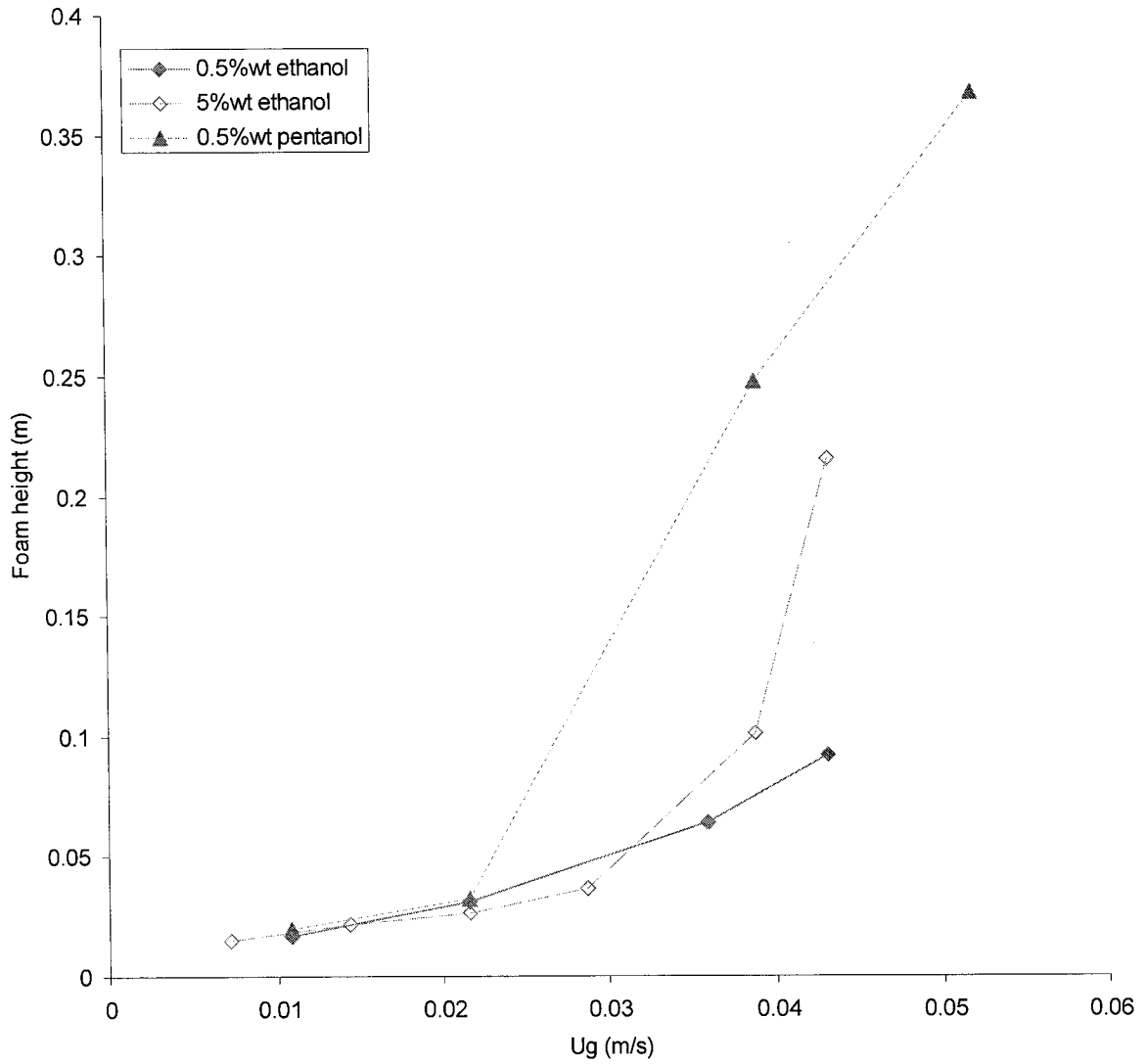


Figure 4.2: Foam heights versus superficial gas velocity for the alcohol solutions.

4.2. Bubble column hydrodynamics

The following sections present bubble column gas holdups and their correlation.

4.2.1 Gas holdup

The average absolute relative difference on gas holdups for repeated experiments (two points) was less than 2%. In addition, when the liquid was batch ($U_L = 0$), the average absolute relative difference between phase holdups obtained from the rise of the liquid level and the dynamic pressure drop were also less than 2%. It is important to note that gas holdups at $U_L = 0$ were obtained in the bubbly liquid below the foam layer.

Figure 4.3 presents the gas holdups for all liquids in the batch and circulating bubble columns. For both operating modes, gas holdups increase with an increase in superficial gas velocity. Gas holdups are always lowest for the tap water. Unfortunately there were no observable trends regarding the nature and concentration of the surface-active agents. Kelkar et al. (1983) found that gas holdups increased with increasing carbon chain length (C_1 - C_4) but that varying the concentration from 0.5 to 2.4% wt. was insignificant. The ethanol concentration was thus varied below to above the c_t value, suggesting that is not an appropriate parameter for modeling purposes. On the other hand, Krishna et al. (2000) notice a monotonic increase in gas holdup with increasing ethanol concentrations from 0.02 to 0.79% wt., which are below c_t . Davis and Acrivos (1966) developed another definition of the critical concentration value above which the effect of surfactant concentration becomes negligible. The definition was based on a criterion to predict the transition between the circulating (Hadamard-Rybcynski) and non-circulating (Stokes-type) internal gas flow in the bubble. The lack of effect alcohol molecular weight on overall gas holdup is somewhat surprising as the pentanol did show greater foaming tendencies than that of the ethanol solutions. Further studies on the specific bubble population would be required to elucidate all these effects. Nonetheless, it is interesting to note gas holdups of all surface-active solutions can be grouped and correlated within +/- 13%. The gas holdups could then potentially be modeled as with or without bubble coalescence inhibition, i.e. without a spectrum.

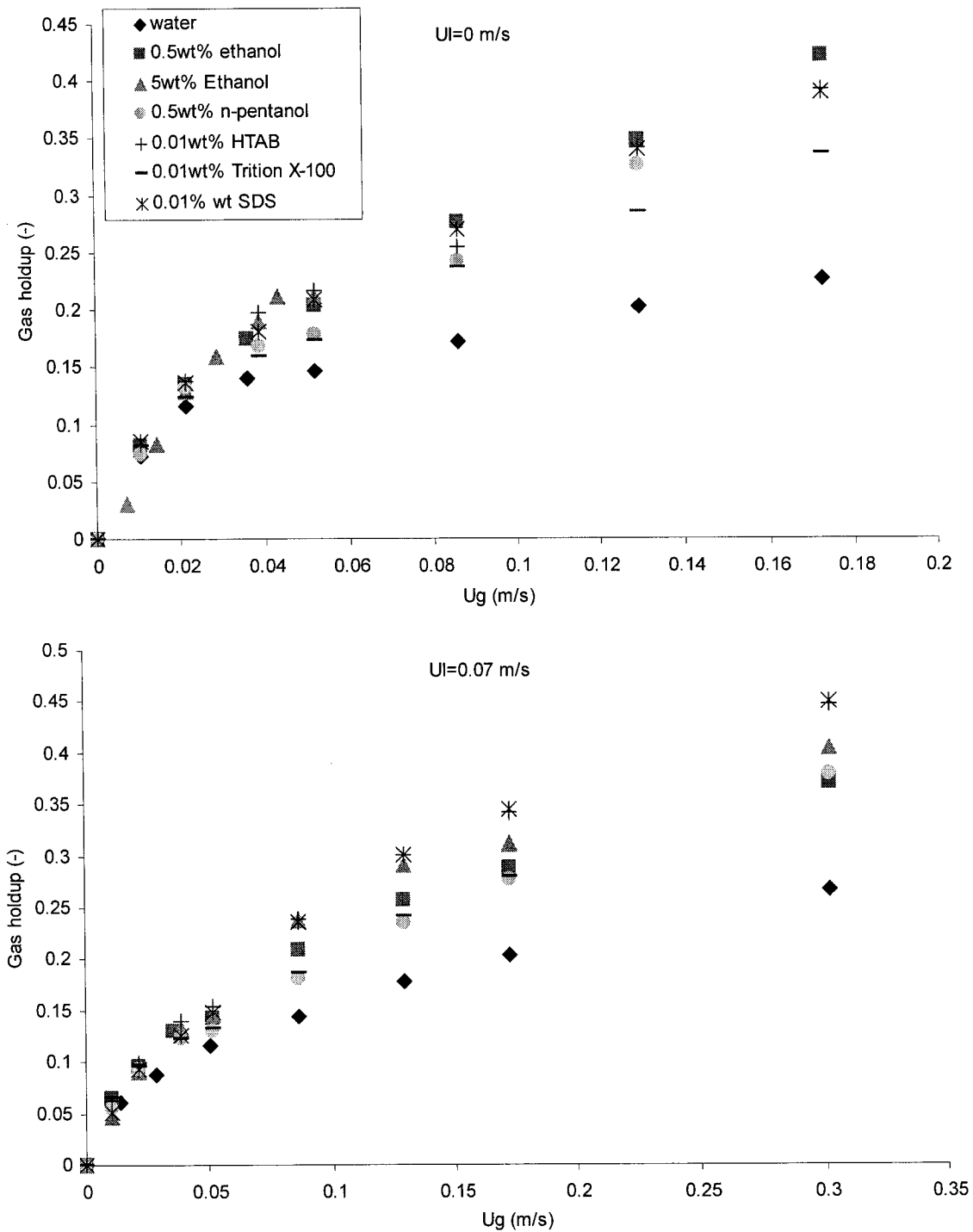


Figure 4.3: Overall gas holdup versus U_g for all liquids in the bubble column at $U_L = 0$ and 0.07 m/s.

The dispersed-to-coalesced bubble flow regime transition is a gradual phenomenon occurring over a gas velocity range. However, a representative regime transition velocity can be taken as the point where the slope changes on the ϵ_g versus U_g graph. As expected,

the presence of surface-active agents delays the transition from dispersed to coalesced bubble flow by inhibiting bubble coalescence with the effect being more obvious at $U_L = 0$. At $U_L = 0$, the regime transition occurs around $U_g = 0.045$ m/s and 0.03 m/s for the surface-active solutions and tap water, respectively. The difference is only marginal due to the presence of natural contaminants (e.g. salts) in the tap water.

The gas holdups of the surface-active solutions are relatively close to those of water in the dispersed bubble flow regime whereas they start to significantly diverge in the transition and coalescence bubble flow regime. As mentioned, the natural contaminants in the tap water inhibited bubble coalescence and reduced bubble rise velocities prolonging the dispersed bubble flow regime and leading to relatively high gas holdups. For spherical and ellipsoidal bubbles ($Eo = g(\rho_L - \rho_g)d_b^2/\sigma < 40$) typically found in the dispersed bubble flow regime, surface impurities eliminate internal circulation of the gas, thereby significantly increasing drag and reducing the rise velocity (Clift et al., 1978). For an air-water system, an Eo number equal to 40 yields a bubble diameter of 17 mm. In the coalesced bubble flow regime, at high bubbling/coalescence rates, tap water seemed to overcome the effect of the contaminants. In this flow regime, large spherical-cap bubbles ($Eo > 40$) form for which liquid inertial forces dominate over surface tension and viscous forces, and the presence of contaminants is thus less important (Clift et al., 1978). The greater difference in gas holdups between the tap water and surface-active solutions in coalesced bubble flow was largely due to the formation of microbubbles ($d_b < 1$ mm) from foaming. As the surface-active solutions underwent a transition to the coalesced bubble flow regime, the intense liquid mixing caused the interface between the foam layer and clear liquid to become fuzzy and eventually disappear resulting in the entire liquid to resemble a froth. The liquid opacity is then due to microbubbles emanating from the gas distributor and from the foam layer, which is now intimately mixed with the frothy liquid. Tap water did not foam.

Figure 4.4 allows a better observation of the effect of liquid flow rate on the gas holdups. The 0.5% wt. ethanol solution was taken as the representative surface-active solution. An increase in liquid superficial velocity decreases the gas holdup with the effect being more

important for the ethanol solution. The decrease in gas holdup with increasing liquid velocity is in large due to the greater relative rise velocities of the bubbles.

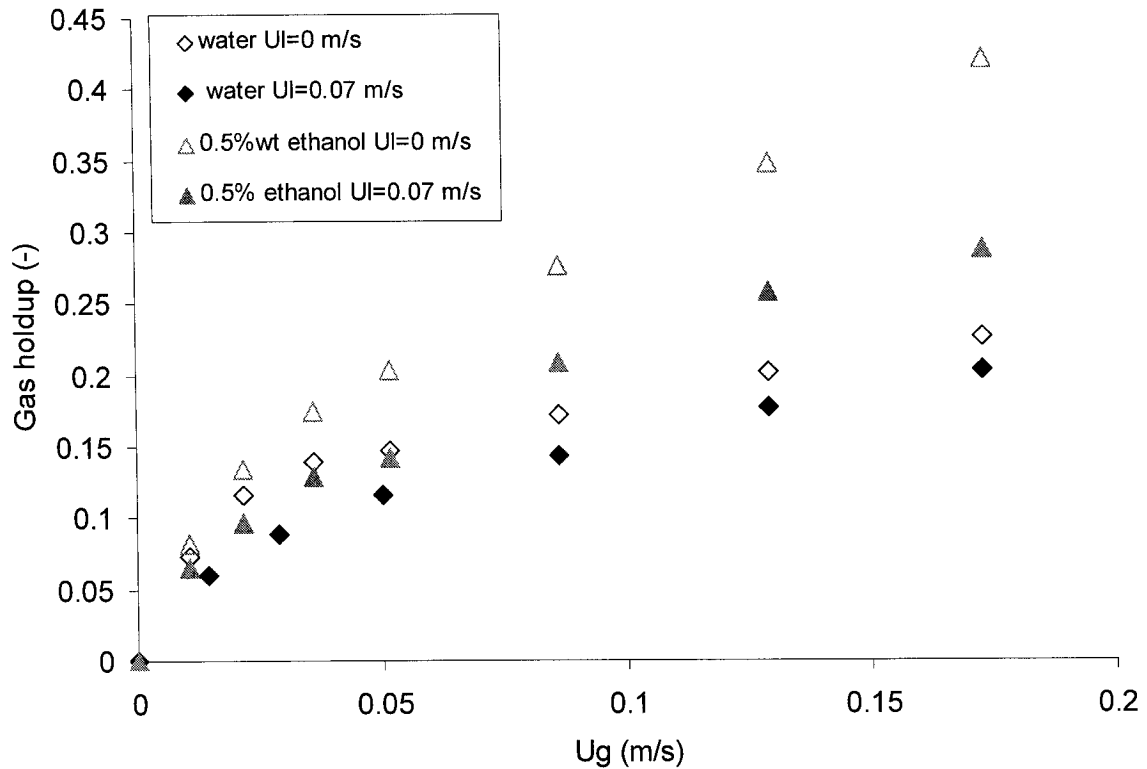


Figure 4.4: Comparison of gas holdup data for water and 0.5% wt. ethanol solution at $U_L=0$ and 0.07m/s.

4.2.2 Correlation of gas holdup data

This section tests the two most widely used bubble column gas holdup correlations as there is insufficient experimental data to propose a novel purely empirical correlation and there still lacks fundamental knowledge for a mechanistic model.

Hikita et al. (1980) developed the following correlation:

$$\varepsilon_g = 0.672\zeta \left(\frac{U_g \mu_L}{\sigma} \right)^{0.578} \left(\frac{\mu_L^4 g}{\sigma^3 \rho_L} \right)^{-0.131} \left(\frac{\rho_g}{\rho_L} \right)^{0.062} \left(\frac{\mu_g}{\mu_L} \right)^{0.107} \quad (4.1)$$

where $\zeta = 1$ for monocomponent liquids and non-electrolyte solutions while for salt solutions ζ is a function of ionic strength. The ranges of dimensionless groups used to develop the correlation are:

$$\begin{aligned} 1.1 \times 10^{-3} < (U_g \mu_L / \sigma) < 8.9 \times 10^{-2} \\ 2.5 \times 10^{-11} < (\mu_L^4 g / \sigma^3 \rho_L) < 1.9 \times 10^{-6} \\ 8.4 \times 10^{-5} < (\rho_g / \rho_L) < 1.9 \times 10^{-3} \\ 1.0 \times 10^{-3} < (\mu_g / \mu_L) < 1.8 \times 10^{-2} \end{aligned}$$

Luo et al. (1999) developed a correlation based on data from a wide variety of gas-liquid systems comprising pure and a few multi-component aqueous and organic liquids, with various gases at several operating pressures. The average absolute error of the predictions is 13% and the maximum error is 53%. The applicable ranges of this gas holdup correlation are summarized in Table 4.2.

$$\frac{\varepsilon_g}{1 - \varepsilon_g} = \frac{2.9 \left(\frac{U_g^4 \rho_g}{\sigma g} \right)^\delta \left(\frac{\rho_g}{\rho_L} \right)^\beta}{\left[\cosh(M^{0.054}) \right]^{4.1}} \quad \text{where } \delta = 0.21M^{0.0079} \quad \text{and } \beta = 0.096M^{-0.011} \quad (4.2)$$

Table 4.2: Applicable range of the Luo et al. (1999) gas holdup correlation.

Parameter (units)	Range
ρ_L (kg/m ³)	668 – 2965
μ_L (Pa·s)	0.0003 – 0.03
σ (N/m)	0.019 – 0.073
ρ_g (kg/m ³)	0.2 – 90
U_g (m/s)	0.05 – 0.69
U_L (m/s)	0 (batch liquid)
D (m)	0.1 – 0.61
H/D	> 5
Distributor types	Perforated plate and bubble caps

Figure 4.5 compares the correlations predictions with the experimental data for tap water and the 0.5% wt. ethanol solution. For water, the correlation of Hikita et al. (1980) consistently underestimates the data while that of Luo et al. (1999) fairs well in the coalesced bubble flow regime where the effects of natural contaminants are no longer pronounced. It is important to note that the discrepancy in the dispersed bubble flow regime can be accentuated by an efficient gas distributor which will produce smaller bubbles leading to greater gas holdups and a delay in the flow regime transition (Vial, 2001). In the present study, the gas distributor holes were relatively small (0.8 mm in diameter) and the pressure drop was sufficiently great to ensure that gas was jetting through all holes at superficial velocities of 0.02 m/s and greater. Both correlations greatly underestimate the gas holdups of the 0.5% wt ethanol solution. This is expected as the liquid physical properties employed in the correlations (density, viscosity, surface tension) are not sufficient to account for the surface-active effects of the alcohol.

Although the surface tension measurements in the tap water did not detect any significant interfacial activity of potential natural contaminants, the relatively high gas holdups were worrisome. Figures 4.6 and 4.7 compare the experimental gas holdups from this study to those of other authors. The data are all similar indicating that our gas holdups in tap water are not unusually high. Furthermore the 0.5% wt. ethanol solution data matches well the data obtained from Kelkar et al. (1983) for both modes of bubble column operation.

We have readjusted the constant ζ in the Hikita et al. (1980) correlation using all of the surface-active liquids. The value of this constant is 1.715 resulting in an average absolute deviation of 14.8% and a bias factor (F_m), defined by equation 4.7, of 0.997. We have also readjusted the constant “2.9” in the Luo et al. (1990) correlation using all of the surface-active liquids. The value of this constant is 5.05 resulting in an average absolute deviation of 11.2% and a bias factor (F_m) of 1.031. Figure 4.8 shows the model predictions versus the experimental data obtained with the 0.5% wt. ethanol solution.

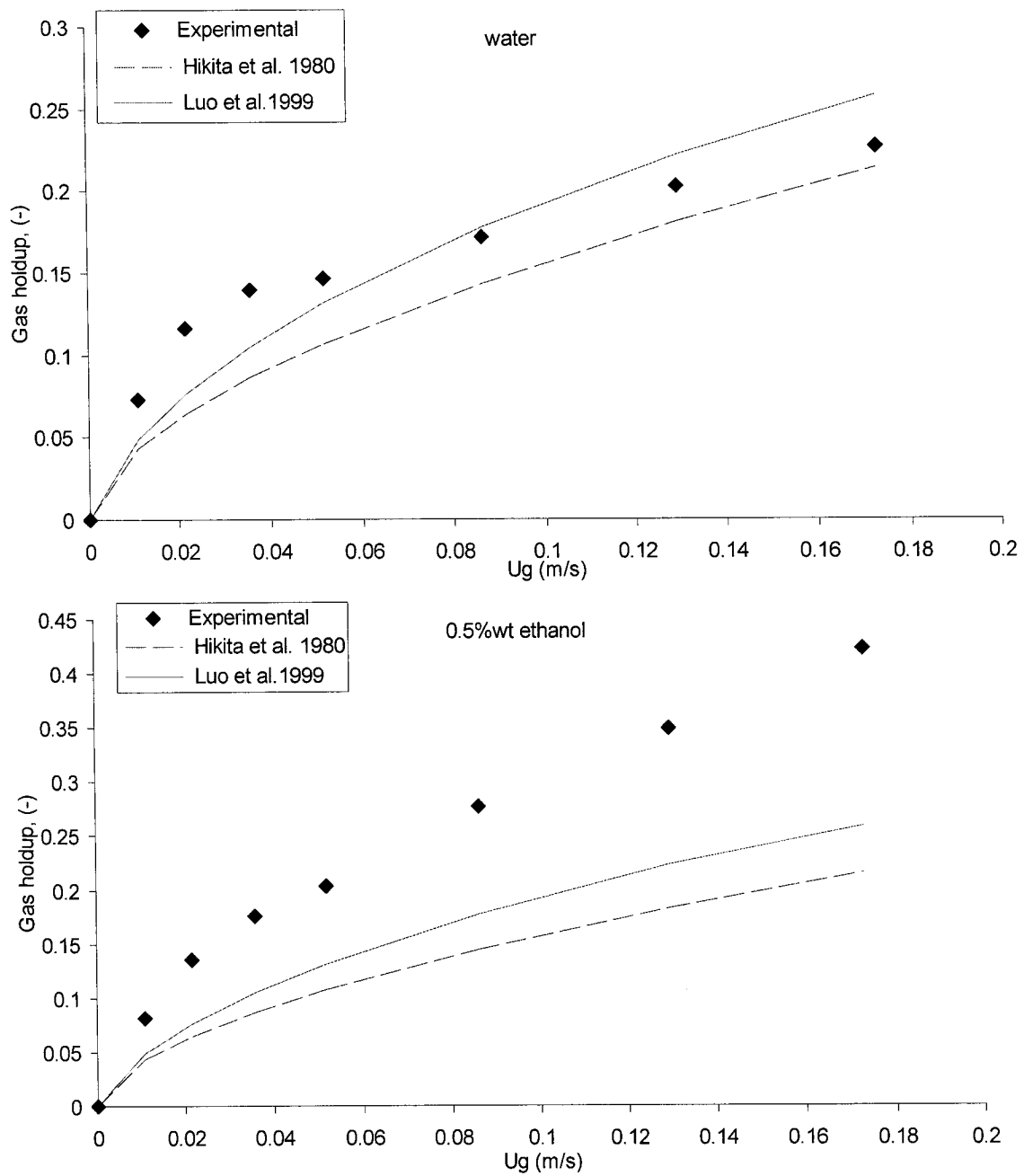


Figure 4.5: Comparison of experimental gas holdups to the predictions of the correlations of Hikita et al. (1980) and Luo et al. (1990) for tap water and 0.5% wt. ethanol solution.

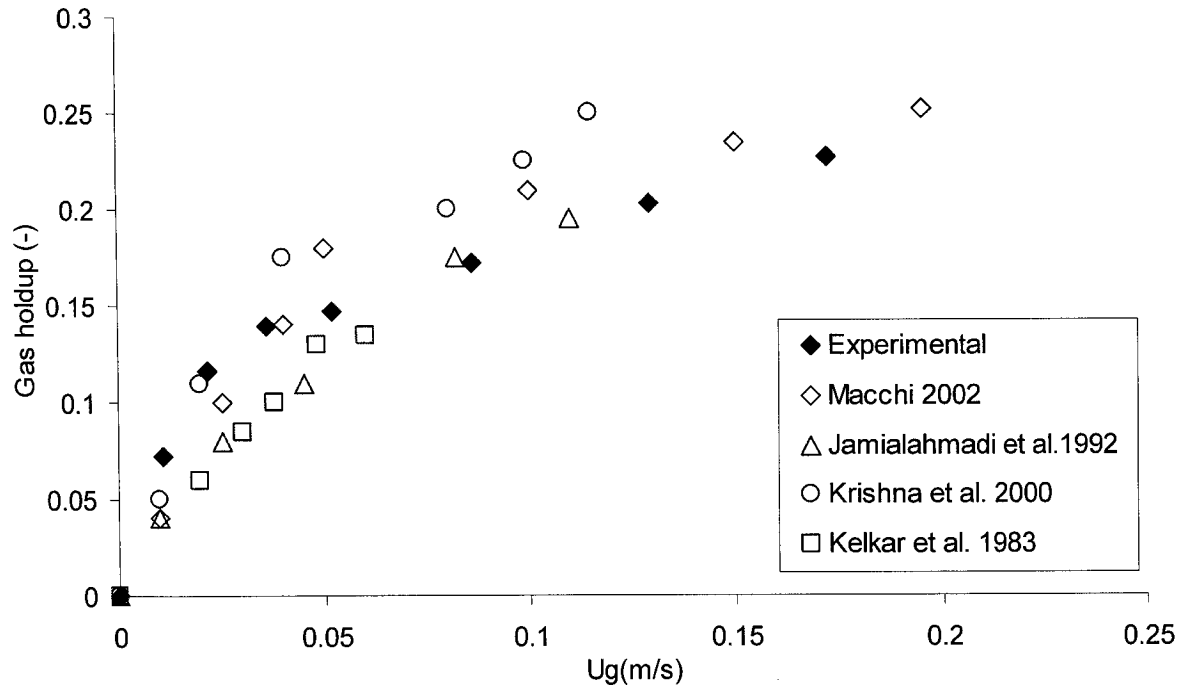


Figure 4.6: Comparison of bubble column gas holdups at $U_L = 0$ for tap water with various literature data.

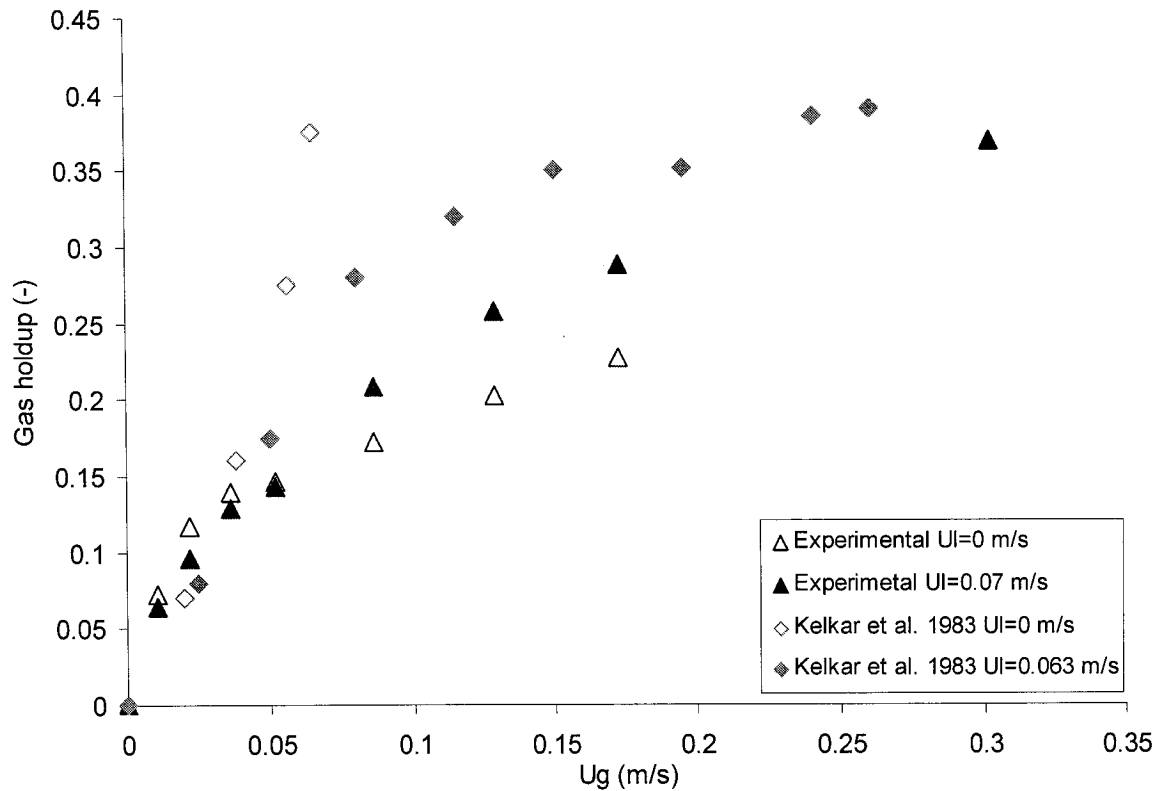


Figure 4.7: Comparison of bubble column gas holdups at $U_L = 0$ and 0.07 m/s for the 0.5% wt. ethanol solution with the data of Kelkar et al. (1983).

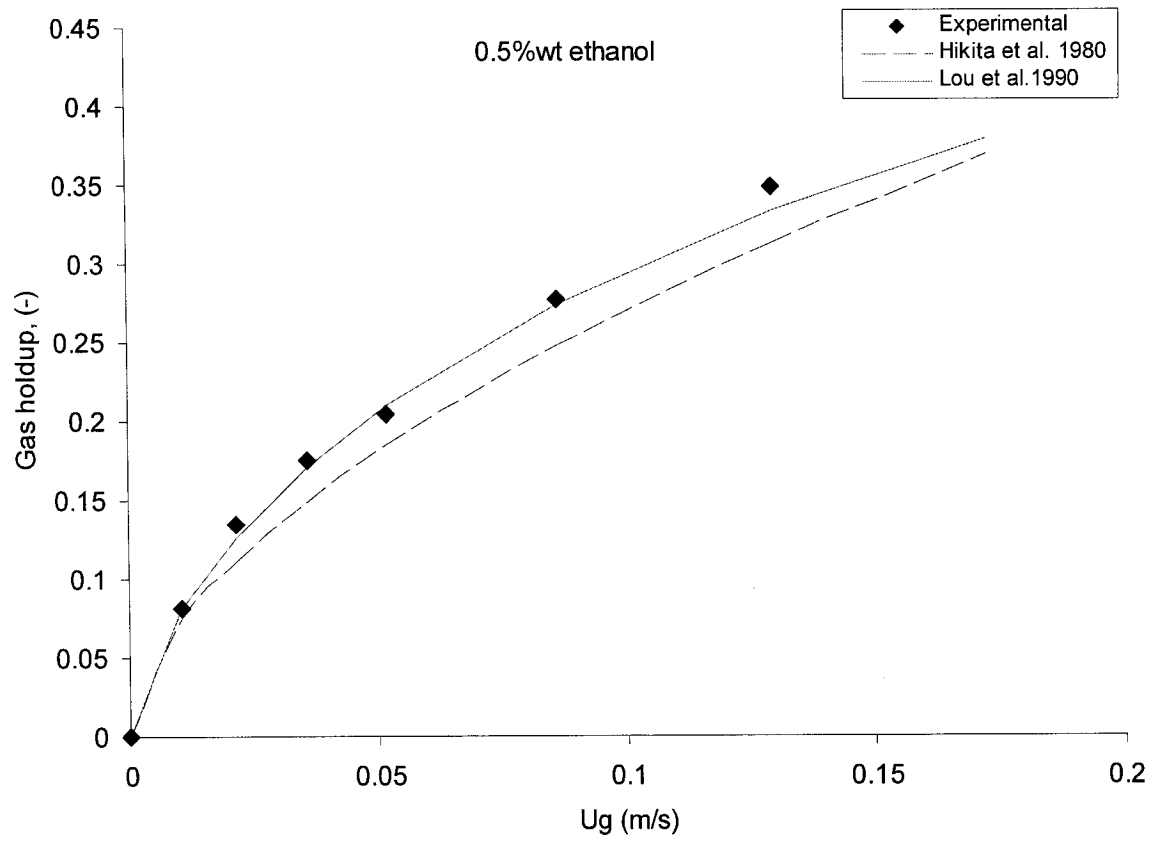


Figure 4.8: Comparison of experimental gas hold-ups to the prediction of the correlations of Hikita et al. (1980) and Luo et al. (1990) after adjusting the constant.

4.3. Three-phase fluidized bed hydrodynamics

This section will first present results for the phase holdups then those obtained for the minimum liquid fluidization velocity.

4.3.1 Overall phase holdups

In the gas-liquid-solid fluidized bed, repeated experiments have been done for water and the 0.5% wt. ethanol solution. The average relative difference between the phase holdups for two repeated experiment with water was less than 5%. Based on this observation, it was assumed that the precision of 5% would also hold for the other liquids. This section will first describe the experiments conducted with the small ($d_p = 1.2$ mm) glass beads followed by those with the large ($d_p = 5$ mm) glass beads.

4.3.1.1 Small glass beads ($d_p = 1.2$ mm)

Figure 4.9 presents the phase holdups of all liquids with the 1.2-mm glass beads at $U_L = 0.0187$ m/s and at several gas velocities. The gas holdup increases with an increase in superficial gas velocity. For all gas flow rates, visually there was a wide distribution of bubble sizes indicating that the flow was transitioning or in the coalesced bubble flow regime. The liquid-solid fluidized bed contracted at the introduction of gas, resulting in an increase in solids holdup and a decrease in liquid holdup. As more gas was introduced into the bed, the gas holdup increased and solid holdup decreased such that the liquid holdup remained relatively constant. The solid holdups correspond to bed expansions of 7 to 25 %.

Gas holdups of the surface-active solutions were again all similar, i.e. can be correlated within +/- 15%, and only slightly greater than that of water. As previously mentioned, bubbles immediately coalesced at the introduction of gas due to the small size of particles and to the relatively high solids holdup. Visually, most bubbles were larger than 17 mm (i.e. $E_o > 40$) suggesting a plausible reason for the relatively small effect of surface-active agents on the overall gas holdups. However, all the surface-active solutions eventually foamed as the gas velocities increased and liquid mixing intensified. Yet, tap water gas holdups were still similar despite not foaming.

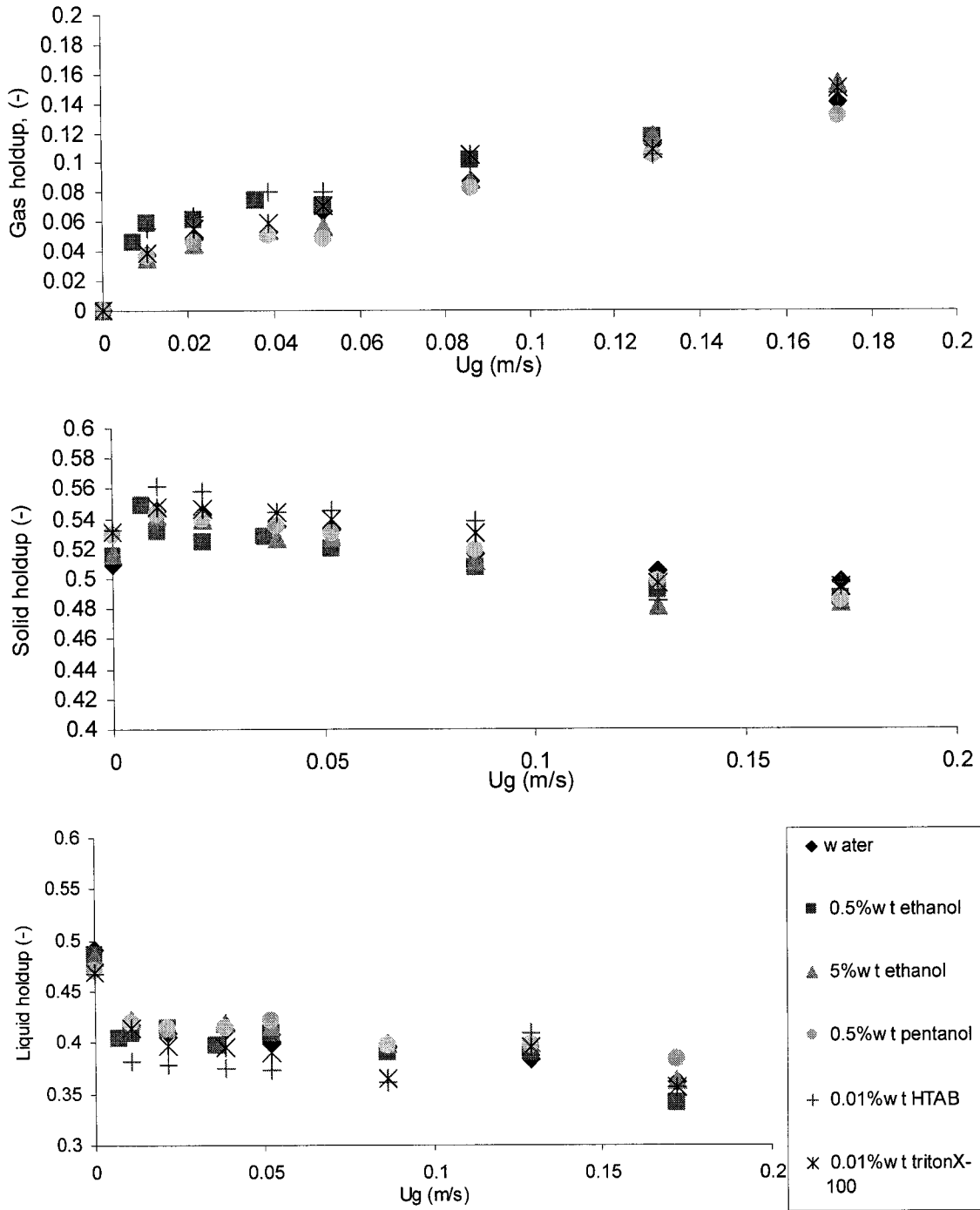


Figure 4.9: Fluidized bed phase holdups versus superficial gas velocity for all liquids at $U_L = 0.0187$ m/s with the 1.2-mm glass beads.

Differences in gas holdups could only be seen in the freeboard above the bed, see figure 4.10. A further analysis on the bubble size distribution would be required to elucidate the impact of particle on the overall bed gas holdup trend. Finally, the increase in gas holdup due to the surface-active agents was sufficiently small that the decrease in solid holdups compensated to keep the liquid holdups similar to water.

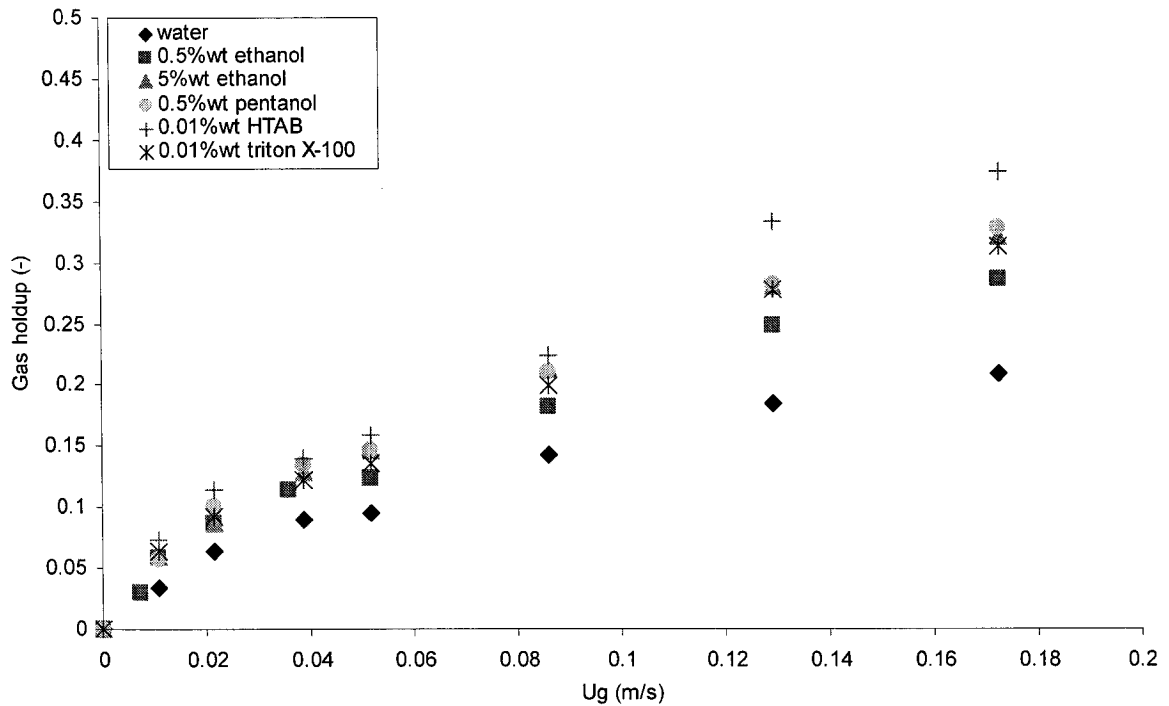


Figure 4.10: Fluidized bed freeboard gas holdups versus superficial gas velocity for all liquids at $U_L = 0.0187$ m/s with the 1.2-mm glass beads.

Figure 4.11 allows determining the effects of surface-active agent at a higher liquid flow rate where the bed expansion is much greater resulting in lower solids holdups. The 0.5% wt. ethanol solution was taken as the representative surface-active solution. Naturally, at a given gas velocity, solids holdups are lower and liquid holdups are greater at the higher liquid velocity. The influence of liquid velocity on gas holdup is usually more subtle. In this case an increase in liquid velocity slightly increases the gas holdup for the ethanol solution while the change is negligible with water. The difference in gas holdups between water and the ethanol solution is therefore greater at the higher liquid velocity.

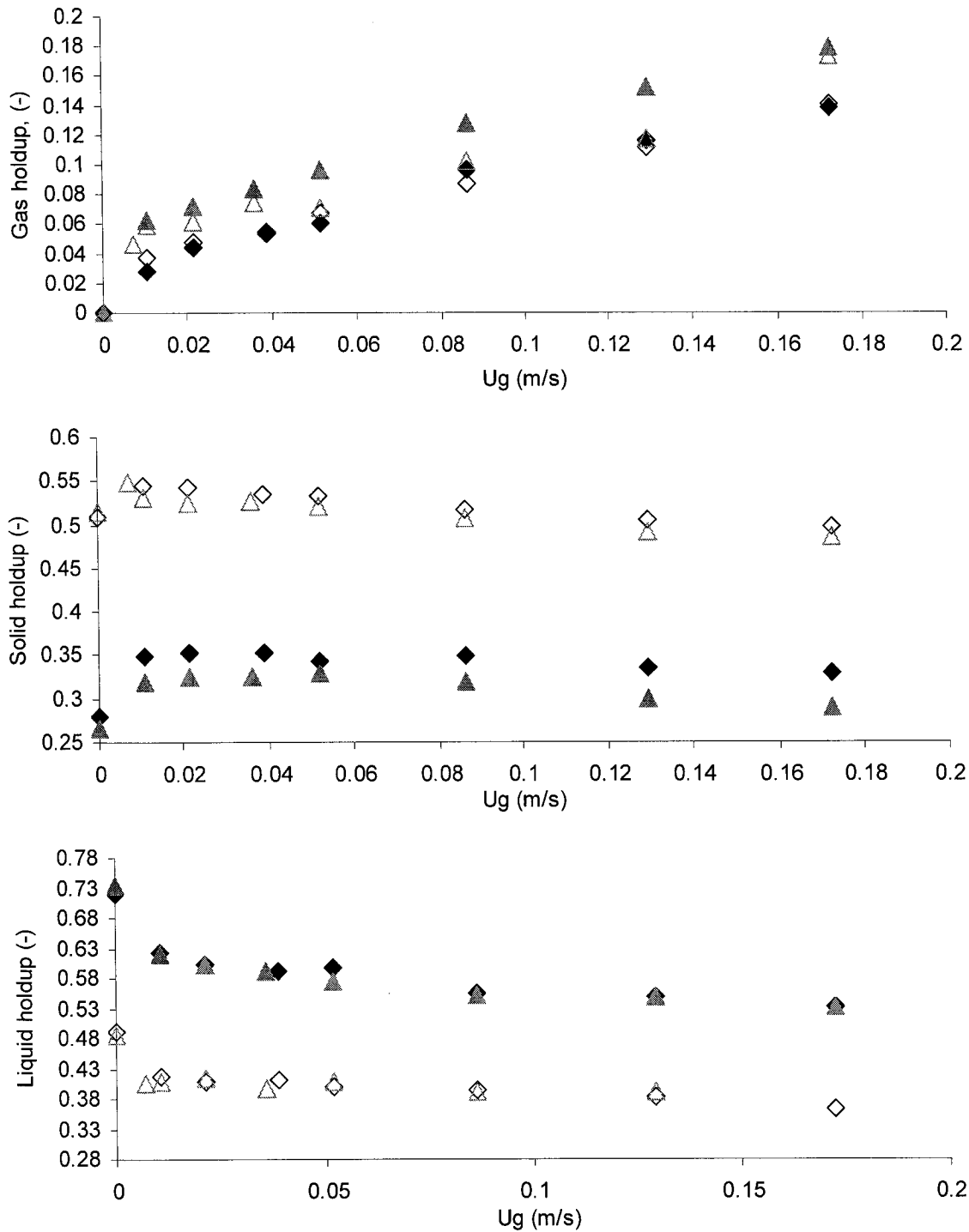


Figure 4.11: Fluidized bed phase holdups versus superficial gas velocity with the 1.2-mm glass beads. Open and closed symbols are for $U_L = 0.0187$ and 0.067 m/s respectively. Diamond and triangle symbols are for tap water and 0.5% wt. ethanol solution respectively.

It would thus seem that the impact of surface-active agents on gas holdups is greater when the bed is more dilute, especially at the higher gas velocities when the ethanol solution is foaming. Tap water again did not foam. At the higher liquid flow rate, it was observed that there were more small bubbles formed possibly due to less particle-bubble interactions allowing the surface-active agents to be active. However, in all cases the bed did contract at the introduction of gas suggesting a coalesced bubble flow regime throughout the experiments. On the other hand, the review of Wild and Poncin (1996) mentioned that a bed that usually contracts at the introduction of gas will no longer do so in the presence of surface-active agents. It is interesting to note that as opposed to the three-phase fluidized bed, an increase in liquid velocity caused the gas holdups to significantly decrease in the bubble column, see figure 4.4.

Figure 4.12 compares the bed and freeboard gas holdups for tap water and the 0.5% wt. ethanol solution at $U_L = 0.0187$ and 0.067 m/s. For both liquids, gas holdups in the freeboard follow the same trend as those in the bed, but are always greater. For both liquid velocities, the difference in gas holdups increases as the gas velocity is increased and the flow becomes more and more turbulent. For a given gas velocity, freeboard gas holdups for both liquids were only marginally lower at the higher liquid velocity. Thus the effect of liquid velocity was somewhat attenuated compared to that observed in the circulating bubble column, see figure 4.4. Finally, as with the bed gas holdups, freeboard gas holdups of the ethanol solution are always greater than those of tap water.

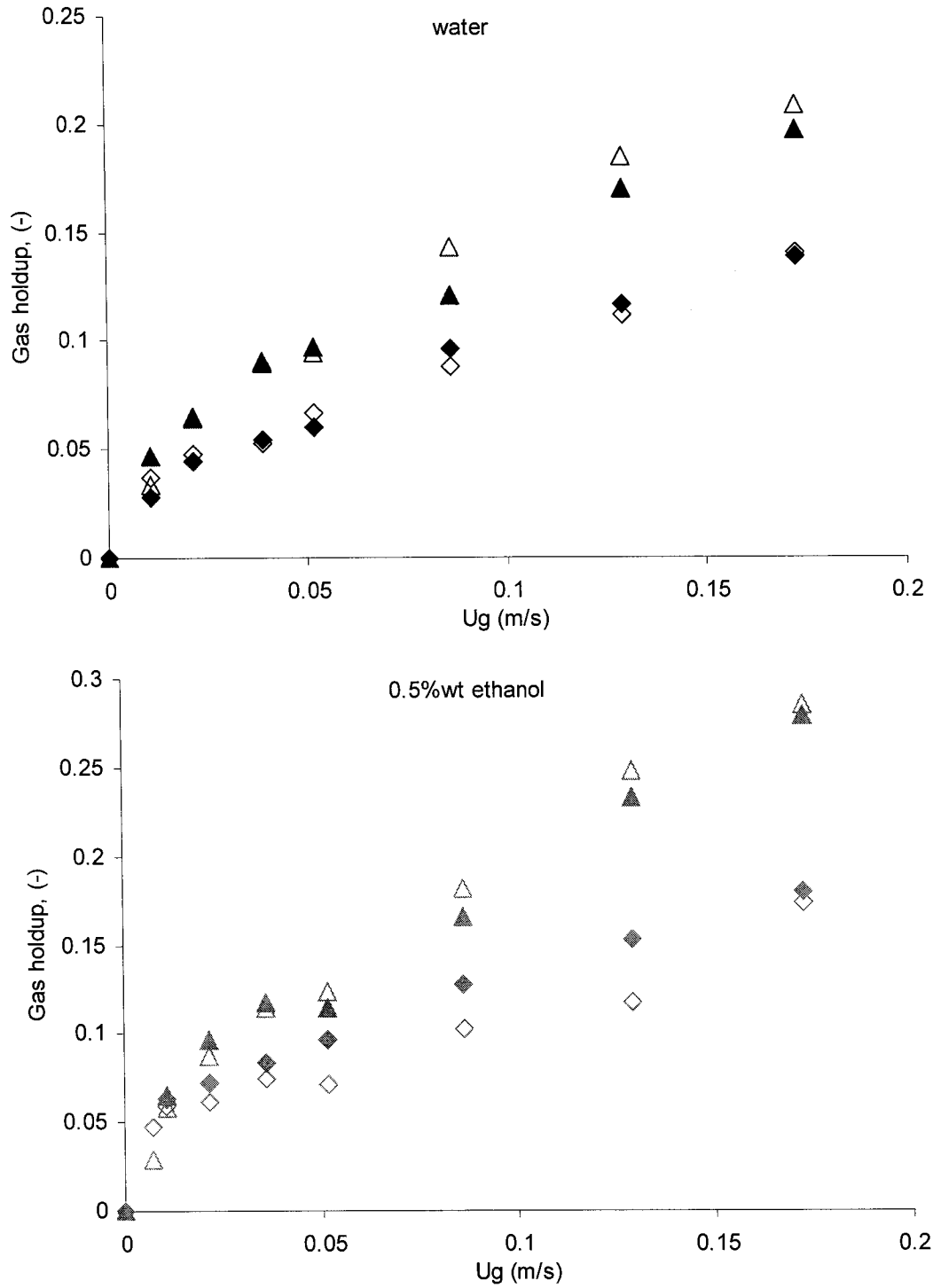


Figure 4.12: Fluidized bed and freeboard gas holdups with the 1.2-mm particles for both water and 0.5% wt. ethanol solution. Diamond and triangle symbols are for the bed and freeboard gas holdups, respectively. Open and closed symbols for $U_L = 0.0187$ and $= 0.067$ m/s, respectively.

4.3.1.2 Large glass beads ($d_p = 5 \text{ mm}$)

Figure 4.13 presents the phase holdups of all liquids with the 5-mm glass beads at $U_L = 0.073 \text{ m/s}$ and at several gas velocities. The liquid-solid fluidized bed expanded at the introduction of gas, resulting in a decrease in solids and liquid holdups. As more gas was introduced into the bed, the gas holdup increased and solid and liquid holdup decreased. The solid holdups correspond to bed expansions of 13 to 62 %.

Gas holdups of all surface-active solutions were similar, i.e. can be correlated within +/- 15%. Gas holdups of the surface-active solutions are similar to those of tap water in the dispersed bubble flow regime and greater than those of tap water in the coalesced bubble flow regime. Further, the dispersed bubble regime was sustained to greater gas velocities for the surface-active solutions. The bubbling pattern resembled that observed in the circulation bubble column where the bubbles were initially well dispersed and then with an increasing gas velocity bubbles started to coalesce and liquid mixing increased causing the liquid to foam. Thus, as with the bubble column, in dispersed bubble flow the natural contaminants in the water affected gas holdups in a similar manner as the selected surface-active agents, while in coalesced bubble flow foaming and microbubbles caused the gas, as well as liquid and solid holdups, to diverge. Tap water again did not foam.

The higher gas holdups in the foaming liquids resulted in both lower solids and liquid holdups compared to those in tap water. To recall, for the smaller particles the increase in gas holdup due to the surface-active agents was sufficiently small that the decrease in solids holdups compensated to keep the liquid holdups similar to water.

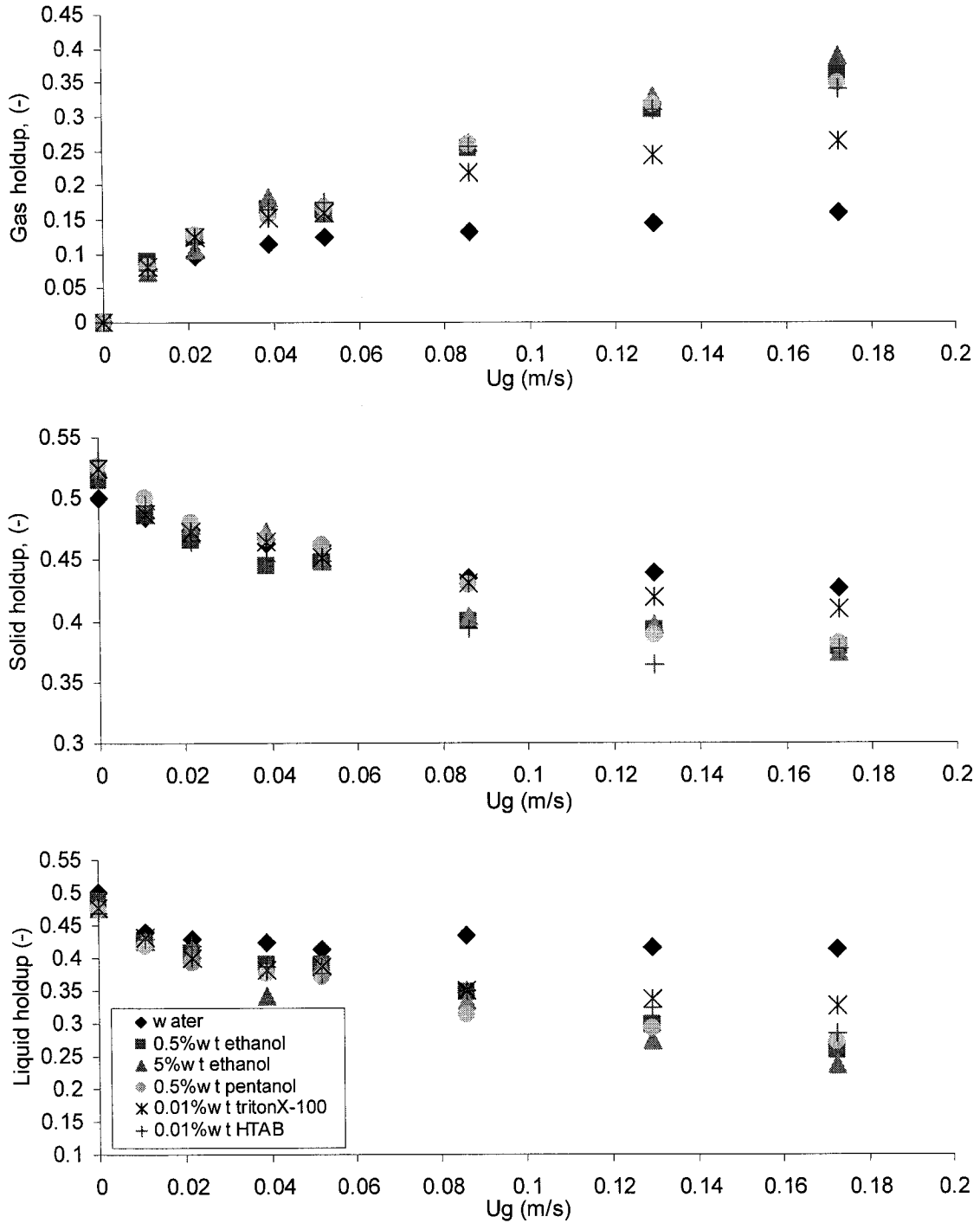


Figure 4.13: Fluidized bed phase holdups versus superficial gas velocity for all liquids at $U_L = 0.073$ m/s with the 5-mm glass beads.

Figure 4.14 allows determining the effects of surface-active agents at a higher liquid flow rate where the solid holdup is much lower. The 0.5% wt. ethanol solution was taken as the representative surface-active solution. Once more, at a given gas velocity, solids holdups are lower and liquid holdups are greater at the higher liquid velocity. The influence of liquid velocity on gas holdup is again more subtle and complex. For the ethanol solution, an increase in liquid velocity slightly decreased the gas holdups as opposed to with the smaller particles but as in the circulating bubble column. For tap water, an increase in liquid velocity causes little change in gas holdup at the low gas velocities whereas there is a significant increase at the higher gas velocities. The change in trend is most likely due to the fact that at the higher liquid flow rate, the dispersed flow regime is prolonged allowing greater gas holdups. This was visually true for all liquids. Because of the delay in flow regime change, gas holdups as well as liquid and solids holdups of the tap water and ethanol solutions were all much closer to each other at the high than at the low liquid velocity.

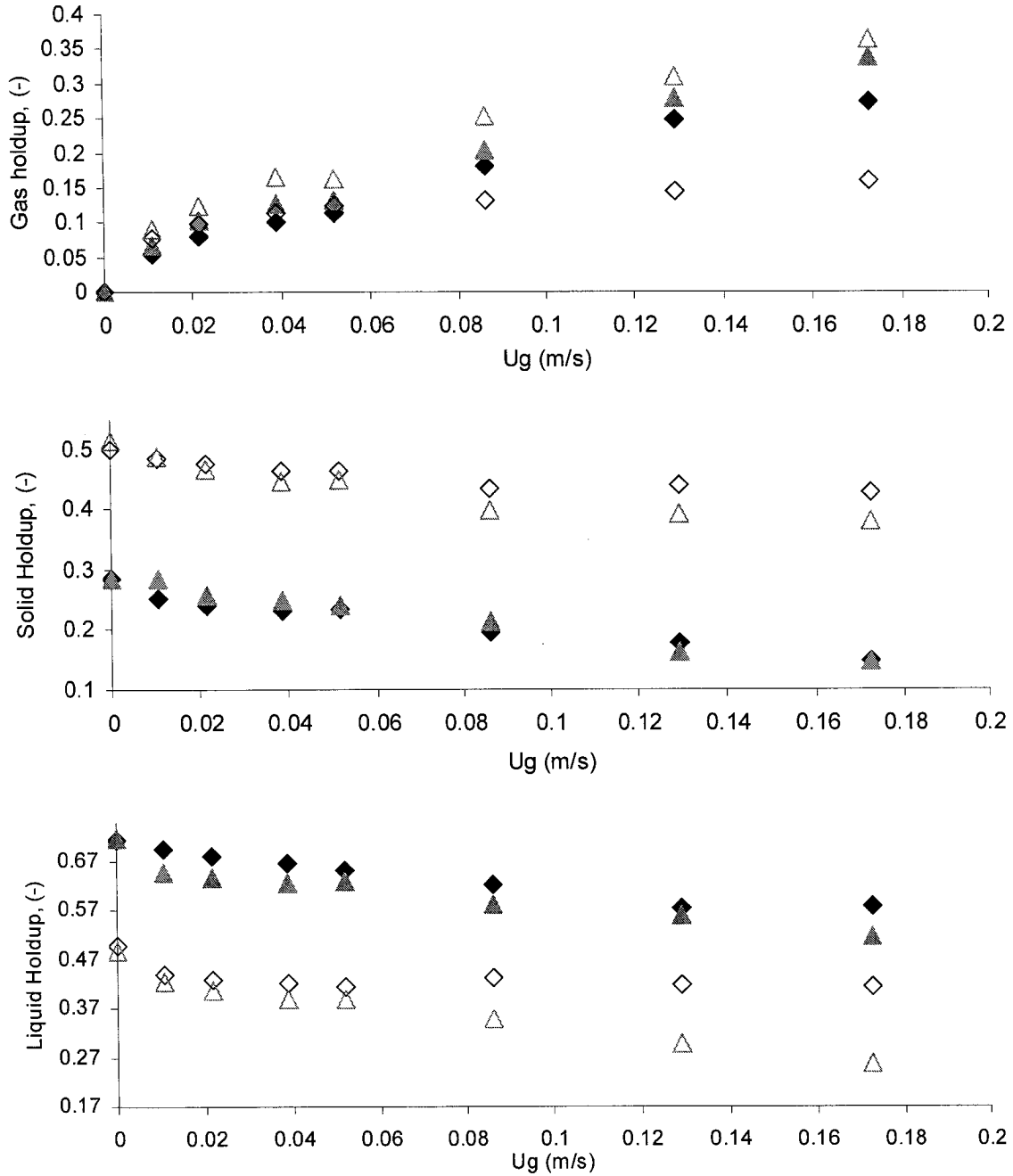


Figure 4.14: Fluidized bed phase holdups versus superficial gas velocity with the 5-mm glass beads. Open and closed symbols are for $U_L = 0.073$ and 0.173 m/s respectively. Diamond and triangle symbols are for tap water and 0.5% wt. ethanol solution respectively.

Figure 4.15 compares the bed and freeboard gas holdups for tap water and the 0.5% wt. ethanol solution at $U_L = 0.073$ and 0.173 m/s. Gas holdups in the freeboard follow the same trend as those in the bed, but are always greater or at least equal. For both liquids, gas holdups in the bed are very similar to those in the freeboard in dispersed bubble flow. Larger deviations between the bed and freeboard gas holdups occur in the coalesced bubble flow regime. To recall, for the small particles there always was a significant difference in gas holdups as the flow regime was always coalesced bubble flow. As with the bed gas holdups, freeboard gas holdups of the ethanol solution are always greater than those of tap water.

It is interesting to note that for both liquids as well as for both particle sizes, there was not a large effect of liquid velocity on the (freeboard-bed) gas holdup difference as long as the flow regime was maintained. This suggests that flow regime and not particle concentration is the main contributing factor to the difference between bed and freeboard gas holdups, although particle concentration may affect the resulting flow regime. This is an important result because at the limit of zero particle concentration, bed and freeboard gas holdups have to be equal for all flow regimes. Is this transition solids concentration really zero? More work is required to elucidate the relationship between bed and freeboard gas holdups.

Figure 4.16 presents the freeboard gas holdup of the 1.2-mm particles, the 5-mm particles and the circulating bubble at U_L around 0.07 m/s. The bubble column and 1.2-mm particle freeboard gas holdups are similar and lower than those of 5-mm particles. This trend is holds true for both water and the ethanol solution. At $U_L = 0.07$ m/s, the bed for the 1.2-mm particles is dilute, closer to the bubble column, whereas for 5-mm particles the bed was still quite dense. The combination of relatively large particle and high solids concentration may have been great enough to break the bubbles in the bed providing a smaller average bubble size entering the freeboard than with the other two systems. However, for the tap water, at higher gas velocities there was no foaming and bubble coalesced readily thus the gas holdups of all three systems converged.

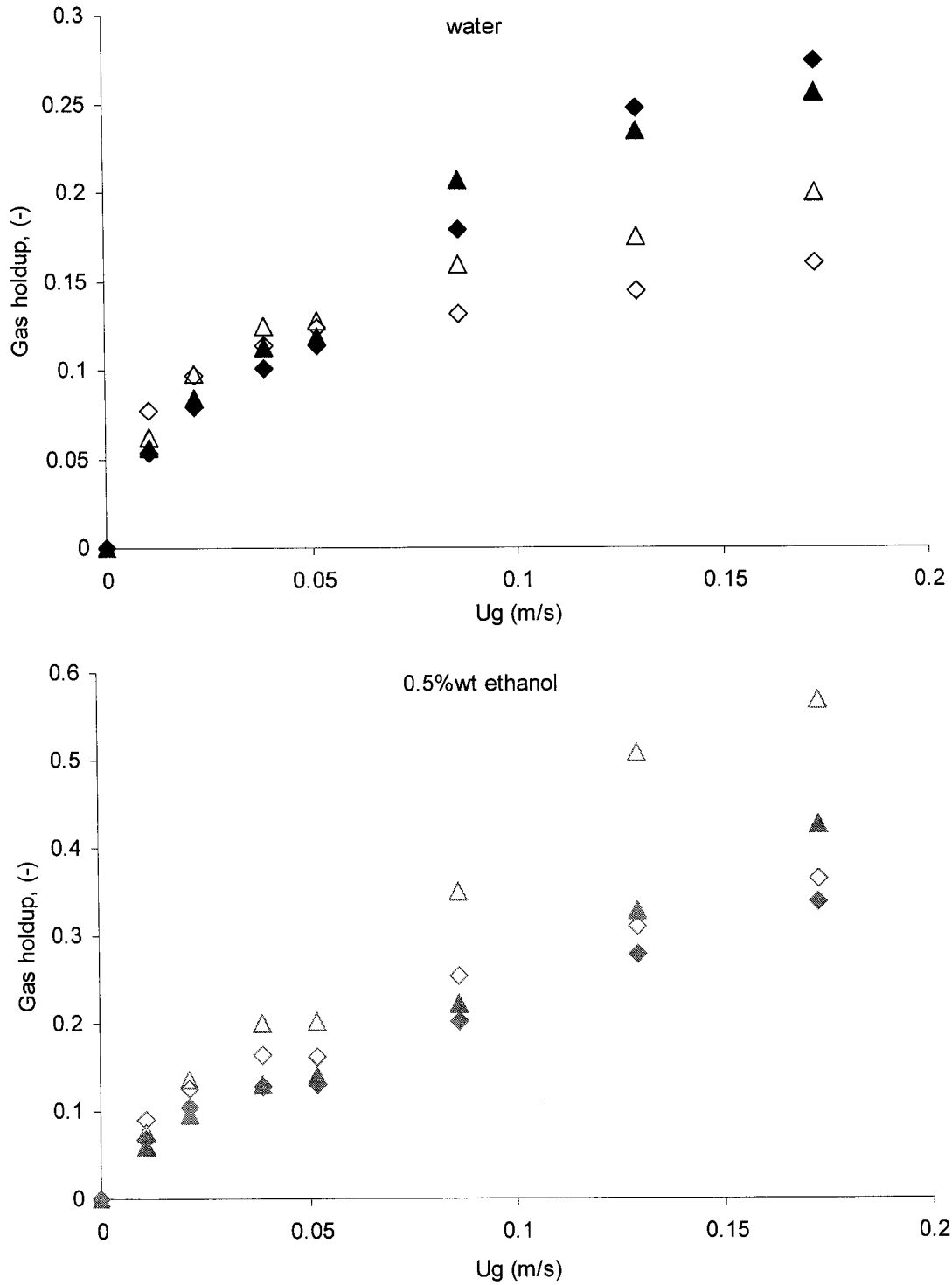


Figure 4.15: Fluidized bed and freeboard gas holdups with the 5-mm particles for both water and 0.5% wt. ethanol solution. Diamond and triangle symbols are for the bed and freeboard gas holdups, respectively. Open and closed symbols for $U_L = 0.73$ and $= 0.173$ m/s, respectively.

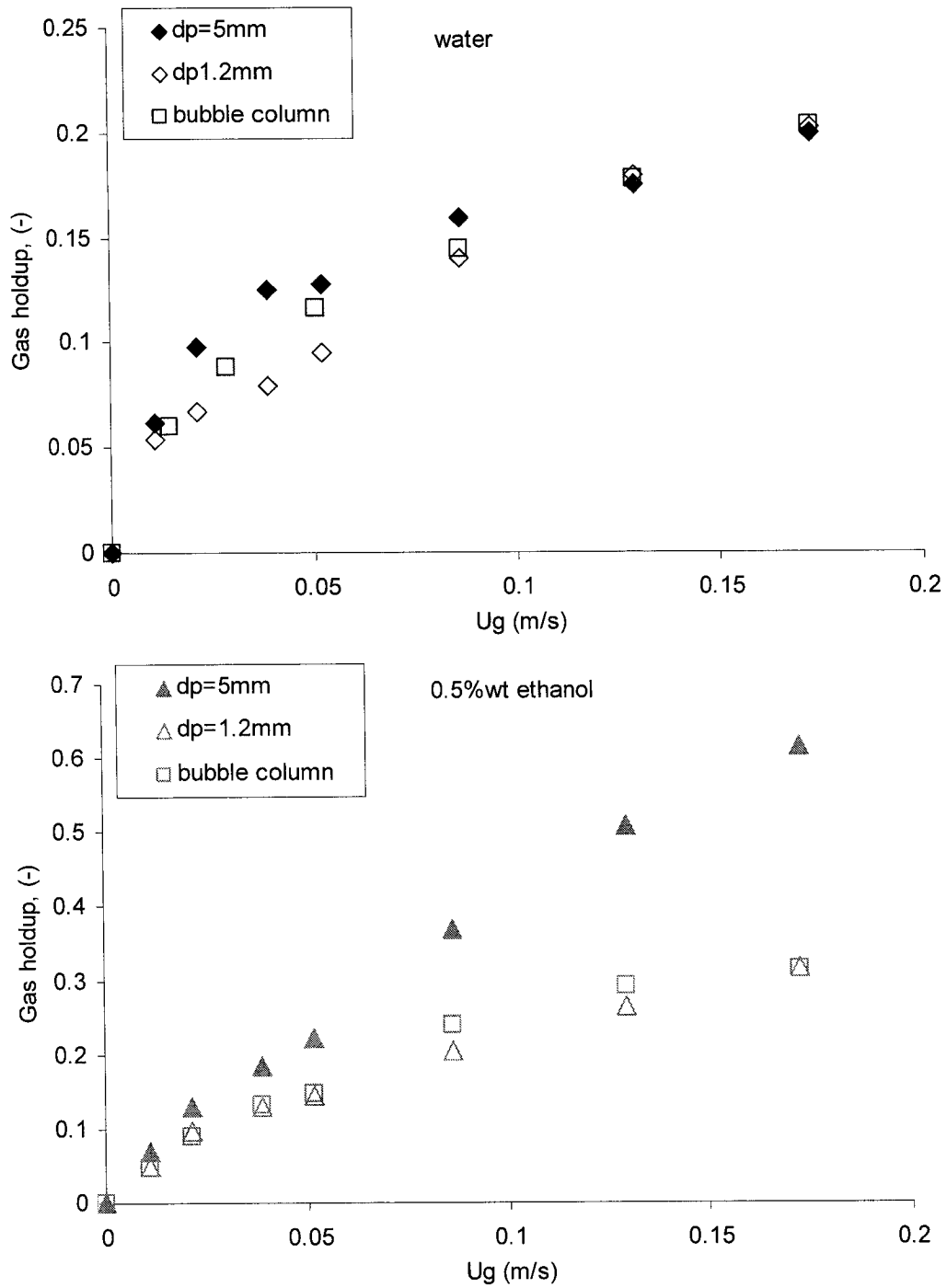


Figure 4.16: Comparison of freeboard gas holdup for particle size 1.2mm and 5mm with bubble column at $U_L=0.07\text{m/s}$ for both water and 0.5%wt ethanol solution.

4.3.1.3 Summary of effects of selected surface-active agents

For the small 1.2-mm glass beads, the following observations were made:

- At low liquid velocity, where the solids holdup was relatively high ($\epsilon_s \approx 0.52$), the selected surface-active agents did not significantly affect the overall gas as well as the liquid and solids holdups. The bed immediately contracted at the introduction of gas leading to coalesced bubble flow and the formation of several large ($E_o > 40$) spherical-cap bubbles, which are not as sensitive to the presence of surfactants. Gas holdups were below 15% for all gas velocities. The surface-active solutions foamed and tap water did not, but phase holdups remained all similar. The trend was more “understandable” in the freeboard where gas holdups of the surface-active solutions differed from those of tap water especially at the higher gas flow rates when the liquids foamed.
- At the high liquid velocity, where the solids holdup was relatively low ($\epsilon_s \approx 0.3$), the selected surface-active agents increased the gas holdups which in turn mainly lowered the solids holdup. In the dilute bed, dispersed bubble flow was not seen as the bed did contract at the introduction of gas, but there were certainly many more spherical or ellipsoidal bubbles for which $E_o < 40$. The impact of foaming was more evident here.

For the large 5-mm glass beads, the following observations were made:

- At low liquid velocity, where the solids holdup was relatively high ($\epsilon_s \approx 0.45$). The bed expanded at the introduction of gas allowing the dispersed bubble flow regime to subsist before transitioning to coalesced bubble as the gas flow was further increased. Effects of the selected surface-active agent were significantly less in the dispersed bubble flow regime due to the presence of natural contaminants in the tap water. In the coalesced bubble flow regime, intense mixing caused the surface-active liquids to foam leading to greater gas holdups which in turn reduced both the liquid and solid holdups.
- At the high liquid velocity, where the solids holdup was relatively low ($\epsilon_s \approx 0.2$), the selected surface-active agents did not significantly affect the phase holdups since the regime remained mainly in dispersed bubble flow where the natural contaminants in the

tap water could be active. At the highest gas velocities, where the flow was transitioning for tap water, larger differences in phase holdups occurred.

Figure 4.17 presents the gas holdups measured by Nacef (1991) in a three-phase fluidized bed of air, water and a 1% wt. ethanol aqueous solution, and glass beads of 1.2 and 4-mm in diameter. The trends are quite similar to those of the present study. For the small glass beads, the effect of surface-active agent was minor, but increased in importance as the liquid velocity increased. For the large glass beads, the effect was minor in dispersed bubble flow but increased as the flow regime reached coalesced bubble flow. The also observed similar effects of liquid flow rate on gas holdups for both their small and large particles.

Finally, it had been mention that the deviations between gas holdups of the surface-active agent solutions were small, i.e. can all be grouped within +/- 15%. Table 4.9 now shows the absolute average deviation (AAD) between the phase holdup data of tap water and the 0.5% wt. ethanol solution. Here the AAD is defined as $ABS((\epsilon_{\text{ethanol}} - \epsilon_{\text{water}})/\epsilon_{\text{water}})$. The values of AAD between the gas holdups in the bubble column and three-phase fluidized bed are similar and reasonable, around 30%. The bed voidage and liquid holdups are hardly influenced by the presence of surface-active agents and this is the reason that most researchers have correlated to these two parameters when modeling the holdups of three-phase fluidized beds.

Table 4.3: AAD between water and 0.5wt% ethanol data for bubble column and three-phase fluidized bed. Here the AAD is defined as $((\epsilon_{\text{ethanol}} - \epsilon_{\text{water}})/\epsilon_{\text{water}})$

System	AAD
Bubble column	
Gas holdup	0.28
Three-phase fluidized bed	
Bed voidage	0.05
Liquid holdup	0.06
Gas holdup	0.25

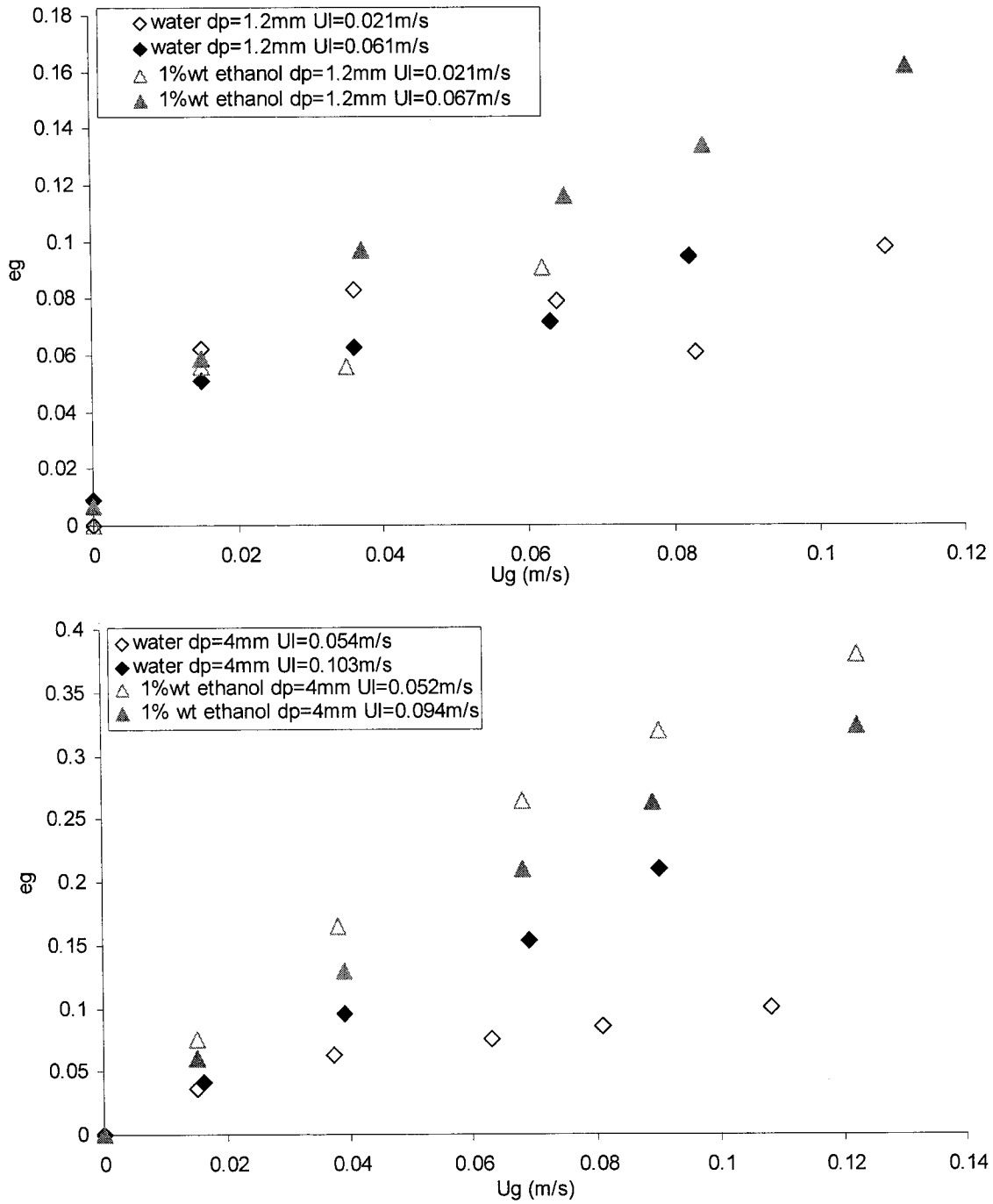


Figure 4.17: Three-phase fluidized bed gas holdups for water and 1%wt ethanol solution and for particle sizes of 1.2-mm and 4-mm from the work of Nacef (1991).

4.3.2 Correlation of phase holdup data

In this section, the most widely used correlations of Han et al. (1990) and Larachi et al. (2001) will be tested.

Based on the tested Richardson and Zaki (1954) equation for liquid-solid fluidized beds, Han et al. (1990) developed correlations to predict the phase holdups in gas-liquid-solid fluidized beds. The liquid holdup correlation was based on 2875 points, while the bed voidage ($\varepsilon = 1 - \varepsilon_s$) correlation used 1946 data points. The average relative errors were 8.7% and 6.4% for the liquid holdup and bed voidage, respectively. Wild and Poncin (1996) noted that more than half of the literature points were obtained in air-water-glass bead systems.

The liquid holdup has been correlated in the following form

$$\varepsilon_L = \left(\frac{U_L}{v_t} \right)^{1/n} \left(1 - 0.374 Fr_g^{0.176} We_m^{-0.173} \right) \quad (4.3)$$

for $0.054 \leq \frac{U_L}{v_t} \leq 0.899$; $0.0000395 \leq Fr_g \leq 2.551$; $0.000918 \leq We_m \leq 5.013$

The correlation for the bed voidage was separated into two categories, according to the expansion or contraction of the bed upon injection of gas into the liquid-solid fluidized bed.

For an initial expansion:

$$\varepsilon = 1 - \varepsilon_s = \left(\frac{U_L}{v_t} \right)^{1/n} \left(1 + 0.123 Fr_g^{0.347} We_m^{0.037} \right) \quad (4.4)$$

for $0.029 \leq \frac{U_L}{v_t} \leq 0.481$; $0.0000173 \leq Fr_g \leq 3.788$; $0.00895 \leq We_m \leq 5.479$

For an initial contraction:

$$\varepsilon = 1 - \varepsilon_s = \left(\frac{U_L}{v_t} \right)^{1/n} \left[0.359 Fr_g^{0.552} We_m^{0.124} + \exp \left\{ - \left(\frac{U_L}{v_t} \right)^{0.305} Fr_g^{0.5} \right\} \right] \quad (4.5)$$

for $0.024 \leq \frac{U_L}{v_t} \leq 0.899$; $0.0000928 \leq Fr_g \leq 2.551$; $0.0000659 \leq We_m \leq 1.529$

Figure 4.18 compares the correlation predictions to the experimental data obtained with the smaller glass beads for which the liquid-solid fluidized bed contracted at the introduction of gas. The model of Han et al. (1990) overestimates the gas holdups at the lower liquid velocity, but at least for water fairs better at the higher liquid velocity. However, at the higher liquid velocity, the predicted trend is bizarre as it does not follow the experimental data which is linear. The trend predicted at the lower liquid velocity is fine.

As expected, since the correlation is based on the liquid's density, viscosity and equilibrium surface tension, it predicts only marginal differences between the water and ethanol solution gas holdups. Further, the correlation actually predicts a decrease in gas holdup with a decrease in surface tension whereas experimentally the opposite is found, even for pure liquids.

Figure 4.19 compares the correlation predictions to the experimental data obtained with the larger glass beads for which the liquid-solid fluidized bed expands at the introduction of gas. The predictions and trends are fairly good for the tap water. However, yet again it predicts a decrease in the gas holdup for a decrease in surface tension.

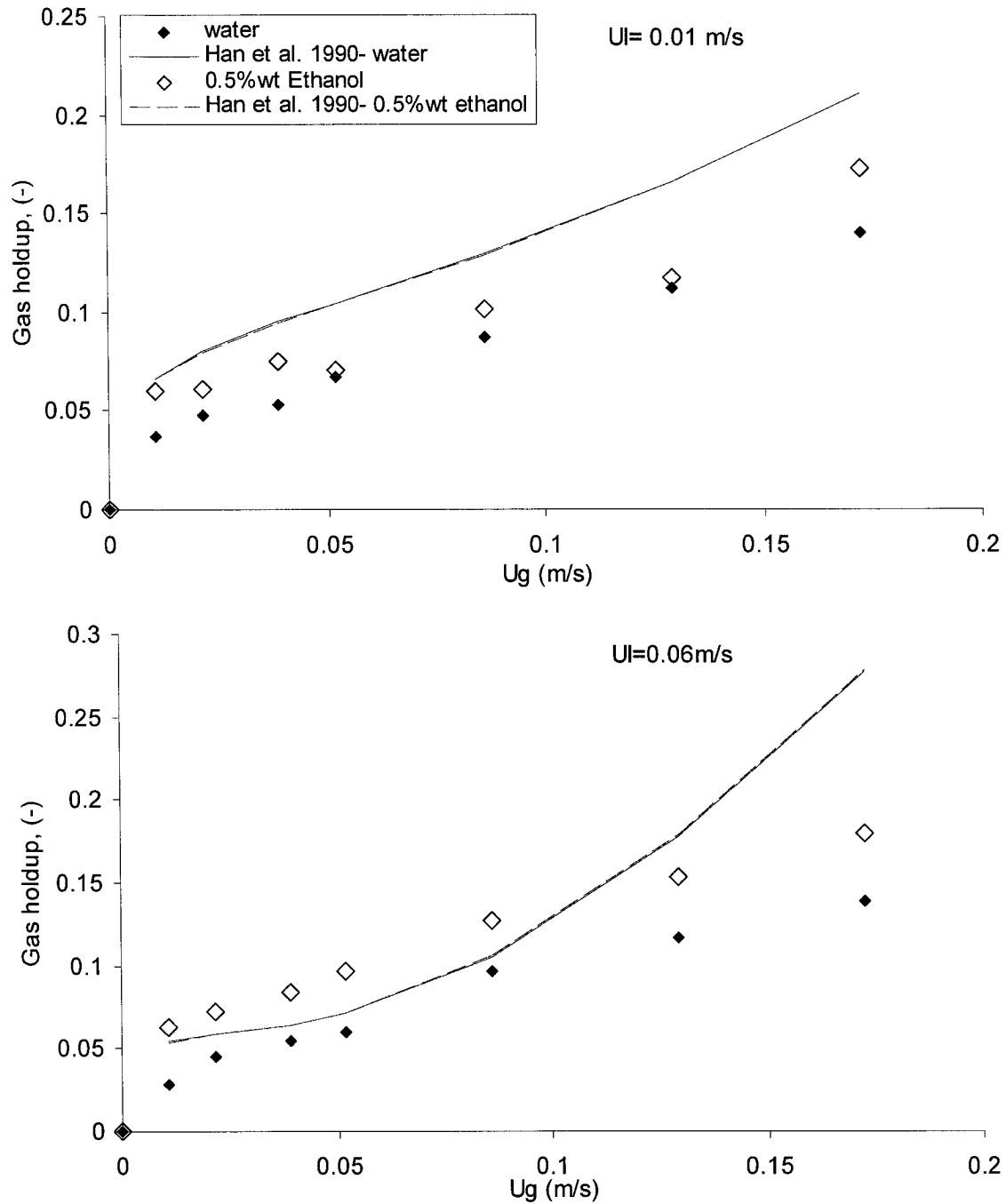


Figure 4.18: Comparison of experimental fluidized bed gas holdups to the predictions of the correlation of Han et al. (1990) for tap water and 0.5% wt. ethanol solution with the 1.2-mm particles at $U_L = 0.0187$ and 0.0677 m/s.

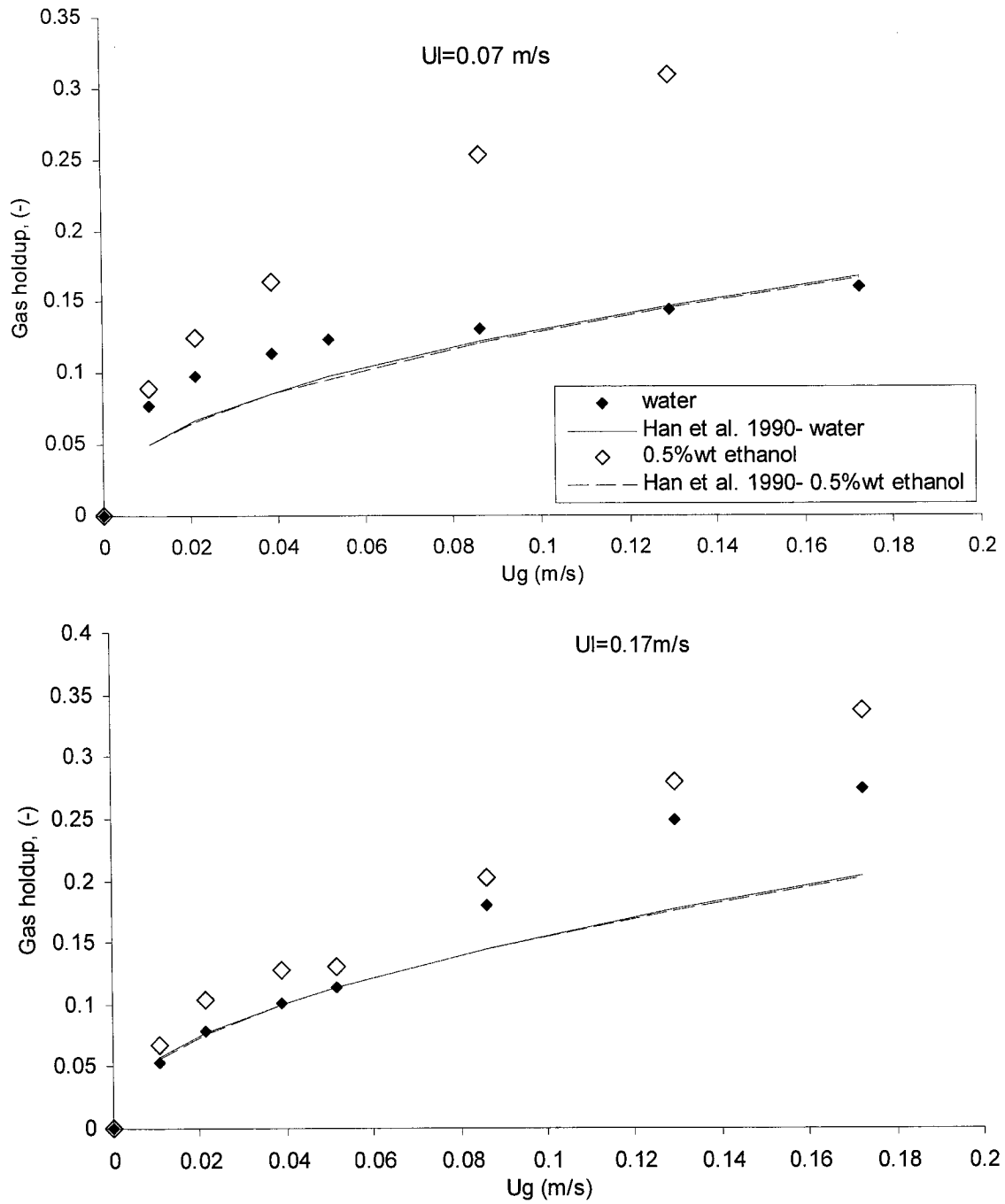


Figure 4.19: Comparison of experimental fluidized bed gas holdups to the predictions of the correlation of Han et al. (1990) for tap water and 0.5% wt. ethanol solution with the 5-mm particles at $U_L = 0.073$ and 0.173 m/s.

The difference between the predicted and experimental phase holdups was quantified with the average absolute deviation (AAD) and bias factor (F_m) which are defined below

$$AAD = \text{ABS}(\varepsilon_{\text{cal}} - \varepsilon_{\text{exp}}) / \varepsilon_{\text{exp}} \quad (4.6)$$

$$F_m = \exp\left(\sum_{i=1}^n \ln(\varepsilon_{\text{cal}} / \varepsilon_{\text{exp}}) / n\right) \quad (4.7)$$

where ε_{cal} is the holdup predicted by the correlation, ε_{exp} is the holdup measured experimentally and n is the number of data points. An ideal correlation will present a bias factor of 1 while values above and below 1 indicate that the model respectively overestimates and underestimates the experimental data. Table 4.4 summarizes the correlation performance. The AAD and bias factor are actually quite good for the solids and liquid holdups whereas the scatter is significant, but reasonable for the gas holdup. The bias for the gas holdup is surprisingly low, but would be significantly greater had individual data sets be taken.

Table 4.4: Average absolute deviation (AAD) and bias factor (F_m) for the Han et al. (1990) correlation based on the experimental phase holdups in figures 4.10 and 4.13

Liquid	Hydrodynamic parameter	AAD	F _m
Water	Bed voidage	0.08	0.967
Water	Liquid holdup	0.08	0.971
Water	Gas holdup	0.34	1.137
0.5% wt. ethanol	Bed voidage	0.12	1.094
0.5% wt. ethanol	Liquid holdup	0.11	0.966
0.5% wt. ethanol	Gas holdup	0.31	0.828

The other widely used literature correlation for three-phase fluidized bed holdups is that developed by Larachi et al. (2001). They combined neural network computing and dimensional analysis to derive complex correlations for the gas, liquid and solids holdups. The data bank used to develop these correlations is impressive as it includes 23,000

measurements taken from about 80 references over the last four decades. Table 4.5 provides the resulting dimensionless groups for each correlation.

Table 4.5: Dimensionless groups used in Larachi et al. (2001) three-phase fluidized bed holdups correlations.

Gas holdup (ε_g)	Liquid holdup (ε_L)	Voidage ($\varepsilon = 1 - \varepsilon_s$)
U_g^2/gd_p	U_L/v_{∞}	U_L^2/gd_p
$U_g\mu_g/\sigma$	$(U_g + U_L)\mu_g/\sigma$	$(U_g + U_L)\rho_L d_p/\mu_L$
$\rho_g U_g^2/\rho_L U_L^2$	$g\mu_L^4/\rho_L\sigma^3$	$(U_g + U_L)\mu_L/g\rho_L d_p^2$
$\mu_L^4/\sigma^2 d_p^2 \rho_L (\rho_p - \rho_L)$	$(\rho_p - \rho_L)/\rho_p$	U_L/v_{∞}
$\phi d_p/D$	$\phi d_p/D$	$g(\rho_p - \rho_L)d_p^2/\sigma$
Coalescence Index (1 = “coalescing liquid”) (2 = “non-coalescing liquid”)	—	$\phi d_p/D$

Larachi et al. (2001) provide a user-friendly Microsoft Excel™ spreadsheet that allows the computation of the phase holdups (see <http://www.gch.ulaval.ca/~flarachi>). It is important to note that there are some fundamental problems in the manner with which the set of correlations was developed:

- There are three independent holdup correlations, which do not always sum to unity. Only two can be truly independent since the sum of phase holdups must give unity.
- The gas density and coalescence index are included solely in the gas holdup correlation, which is wrong as the liquid and/or solids holdups must also be affected.
- The authors propose a binary coalescence index (non-coalescing or coalescing liquid) but fail to mention which types of liquids are non-coalescing and more importantly

under which operating conditions do these liquids foam or at least show bubble coalescence inhibition.

The correlation average absolute deviation and bias factor are given in table 4.6 for the data of figures 4.11 and 4.14. For both liquids, the correlation was disappointing as it did not fare better than the correlation proposed by Han et al. (1990). It underestimated the gas holdups of water, which may be reasonable since the tap water contained some natural contaminants. However, using the coalescence index, it grossly overestimated the gas holdups from the 0.5% wt. ethanol solution. Finally there must have been something wrong with the simulation for the bed voidage.

Table 4.6: Average absolute deviation (AAD) and bias factor (F_m) for the Larachi et al. (2001) correlation based on the experimental phase holdups in figures 4.10 and 4.13.

Liquid	Hydrodynamic parameter	AAD	Fm
Water	Bed voidage	0.99	1.702
Water	Liquid holdup	0.06	1.038
Water	Gas holdup	0.35	0.624
0.5% wt. ethanol	Bed voidage	1.10	1.833
0.5% wt. ethanol	Liquid holdup	0.07	1.073
0.5% wt. ethanol	Gas holdup	0.50	1.231

Finally, the low, medium, high gas holdup correlations of Gorowara and Fan (1990) were not tested because the surface-active liquids presented similar gas holdups despite being part of different liquid categories and hence associated to different gas holdup correlations. Furthermore, it was hypothesized that this approach may be more appropriate in the dispersed bubble flow regime. However, it is in this regime that gas holdups in the tap water were closest to those of the surface-active solutions due to the presence of natural contaminants, which were not detected by the dynamics surface tension experiments. This again invalidates the approach.

4.3.3 Minimum liquid fluidization velocity

Figure 4.20 presents the effect of gas velocity on the minimum liquid fluidization velocity for several liquids and for both the small and large glass beads. Ru_{LM} is the ratio of minimum liquid fluidization of gas-liquid-solid to liquid-solid fluidized bed. The introduction of gas to the bed reduces the available volume for the liquid to flow. If particles are mainly fluidized by the drag force exerted by the liquid, the addition of gas will cause the bed to fluidize at a lower superficial liquid velocity. However, the effect of gas velocity on the minimum liquid fluidization velocity eventually wears off.

There was no significant effect of surface-active agents on the values of U_{Lmf} for the small 1.2-mm particles. As previously mentioned, relatively large bubbles were formed for which the effects of surfactants are small. Further there was not a large difference in gas holdups at $U_L = 0.0187$ m/s (high solids holdup) suggesting that the phase holdups of the liquids should be all similar at U_{Lmf} . Thus, the value of U_{Lmf} would be similar since the viscosity and densities of the liquids are also similar. The effect of surface-active agent seemed to be more pronounced for the larger glass beads as there are more capable of keeping the bubble size sufficiently small for which the surfactants can be active. However, there was not a large difference in gas holdups at $U_L = 0.073$ cm/s (high solids holdup) again suggesting that the phase holdups between liquids should be similar around U_{Lmf} . Perhaps, the differences in U_{Lmf} are due to the presence of microbubbles surrounding the particles which contribute more to particle buoyancy than to overall gas holdup.

The lines in figure 4.20 are the predictions of the liquid-buoyed/gas-perturbed model from Zhang et al (1995). This model is one of the most widely used and assumes that full support of the solids is provided by the liquid, the velocity of which is increased by the presence of the gas. Since the model is not sensitive to the small changes in liquid physical properties, only the predictions of tap water are plotted.

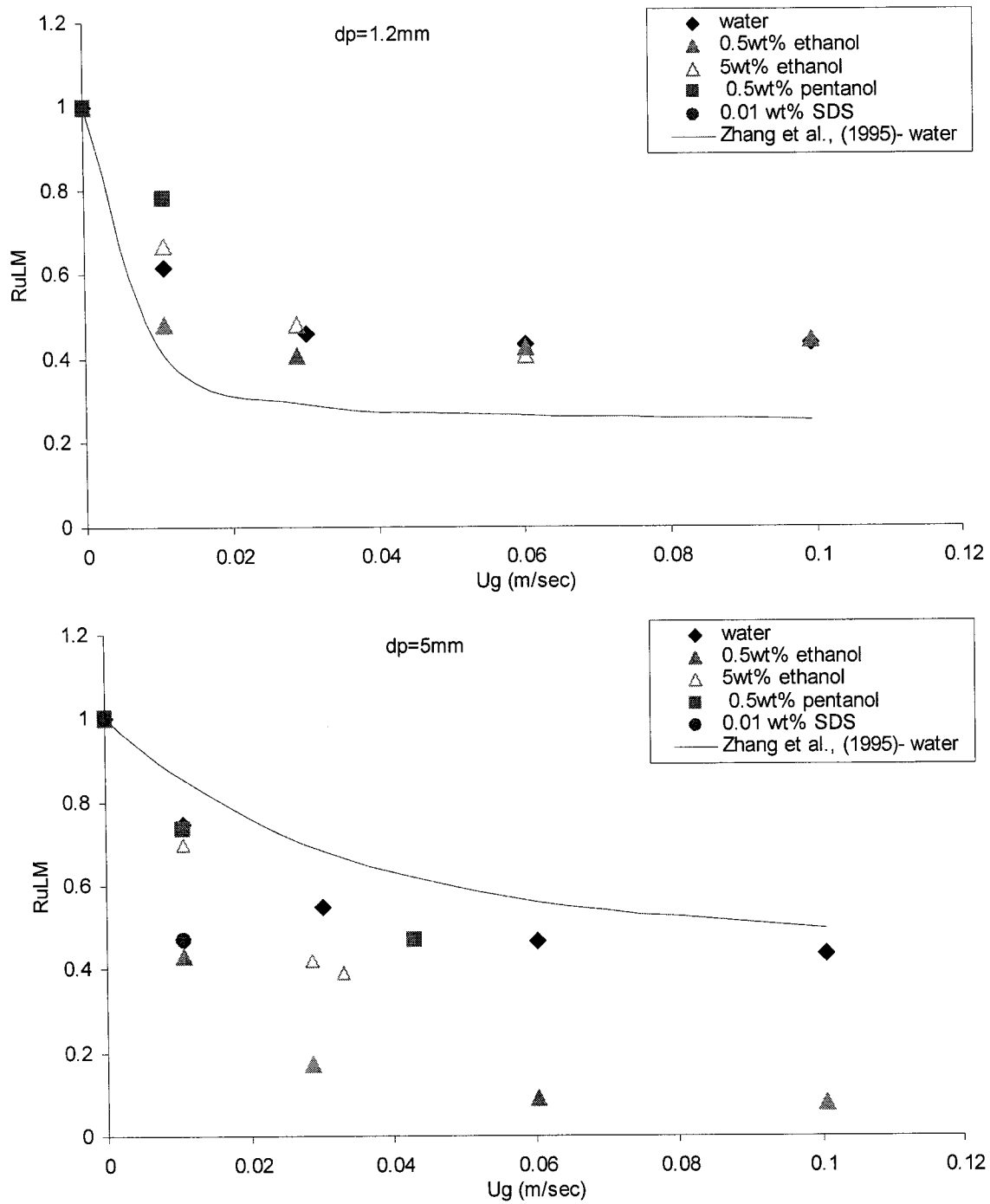


Figure: 4.20 Minimum liquid fluidization velocity versus superficial gas velocity for several liquids and for the 1.2 and 5-mm glass beads.

The model is relatively accurate for the water data with the 5-mm particles. Minimum liquid fluidization velocity for particles larger than 1 mm in diameter should be well predicted by the Liquid-buoyed/gas-perturbed liquid model. However, the model is more suitable to be applied to systems where bubble or wake induced flow is insignificant. Here, with the 1.2-mm particles, large bubbles were formed which may have sucked in its wake some of the liquid required to fluidize the bed. It was difficult to obtain the minimum liquid fluidization velocity in the surface-active solutions since at low liquid velocity the pressure drop through the distributor may have not been sufficient to evenly distribute the liquid across the column cross-section.

Finally figure 4.21 presents the experimental results of Nacef (1991) who used a system composed of air, water and 1% wt. aqueous ethanol solution, and 1.2, 2 and 4-mm glass beads. As in the present study, the capability of the surface-active agent to reduce the minimum liquid fluidization velocity increased as the particle size increased.

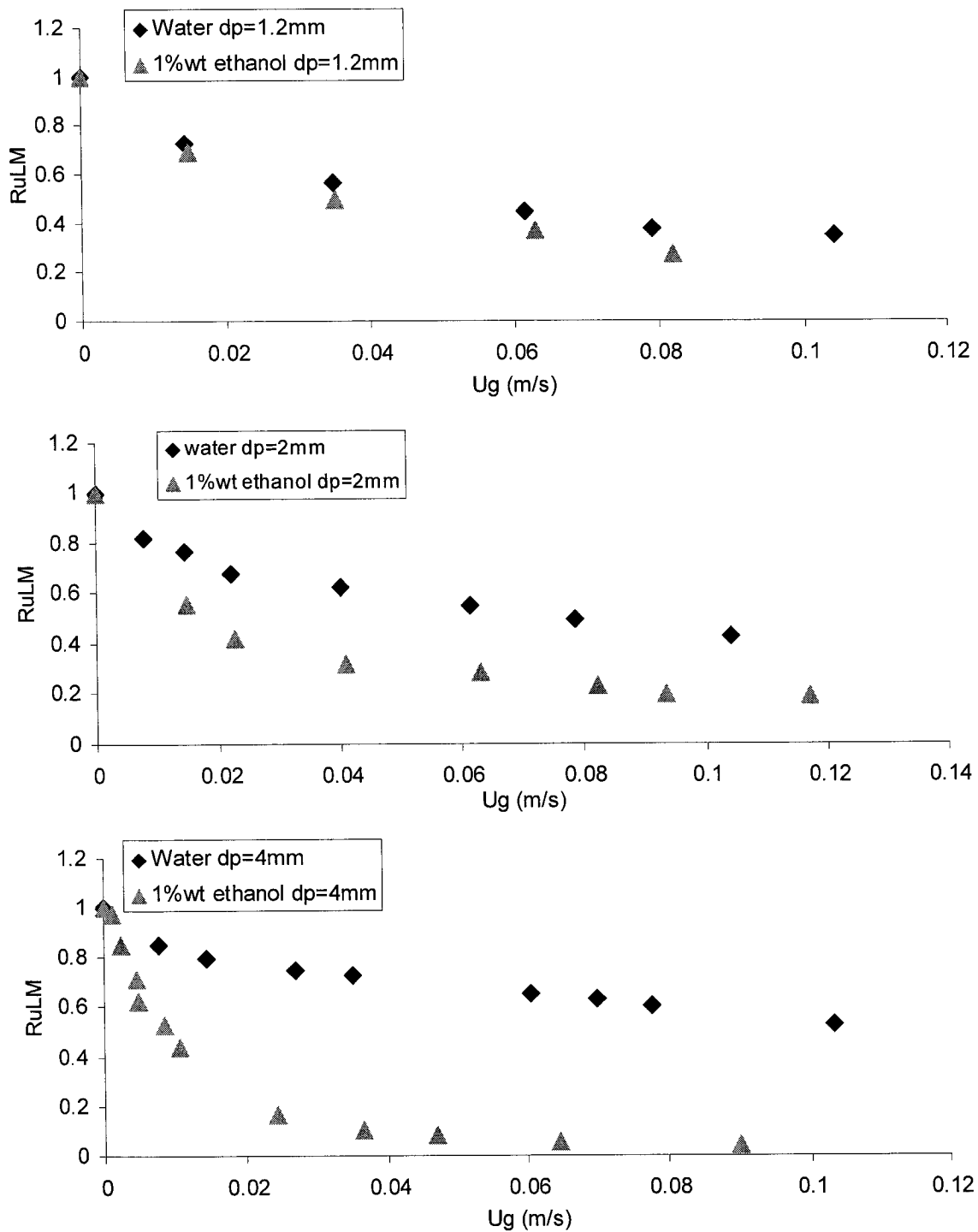


Figure 4.21: Minimum liquid fluidization velocity versus superficial gas velocity for several liquids and for the 1.2, 2 and 4-mm glass beads for various liquids from Nacef (1991).

5. General conclusions and recommendations

This research work aimed to evaluate the effects of surface-active agents on the phase holdups and flow regime transition velocities of gas-liquid bubble columns and gas-liquid-solid fluidized beds. It was also desired to establish the relationship between the bed and freeboard gas holdups in a three-phase fluidized bed. Finally, the promising empirical approach of Gorowara and Fan (1990) to estimate gas holdups was tested.

Bubbles must be below a certain size ($E_o < 40$), which is equivalent to 17 mm in diameter for an air-water system) in order for surface-active agents to have an appreciable effect. One must then look into the operating conditions (gas and liquid superficial velocities, particle size and density, gas distributor) which favour such conditions. This reasoning would lead to surface-active agents having the greatest effect in the dispersed bubble flow regime. However, as was shown, the coalesced bubble flow regime may be subject to the effects of surface-active agents due to the foaming and the formation of several microbubbles ($d_b < 1$ mm). For the present study, holdups in the tap water differed most in the coalesced bubble flow regime because the natural contaminants were not sufficiently active to induce foaming.

For all operating conditions, gas holdups in the freeboard were always equal or greater than those in the bed. It would seem that gas holdups are similar in dispersed bubble flow while they substantially differ in coalesced bubble flow. As with the bed gas holdups, freeboard gas holdups of the surface-active solutions were always greater than those of tap water. These results are important as there are commercial processes (e.g. LC-Finer from Syncude Canada Ltd.) that use the freeboard gas holdup to estimate the bed gas holdup.

The capability of the surface-active agents to reduce the minimum liquid fluidization velocity seemed to increase as the particle size increased. The exact mechanism is not thoroughly understood as there was scatter in the data as well as there were no obvious differences in the phases holdups at minimum fluidization velocity which would have lead to changes in the drag force on the particles. Perhaps, the presence of microbubbles

surrounding the particles contributed more to particle buoyancy than to overall gas holdup. The widely used model of Zhang et al. (1995) represented fairly well the water data but could not account for the presence of surface-active agents.

The deviations between gas holdups of the surface-active agent solutions were small, i.e. can all be grouped within +/- 15%. Moreover, gas holdups of the surface-active solutions were on average only 30% greater than those of tap water. Even with such conditions, the widely used correlation of Han et al. (1990) was adequate for predicting the gas holdups in water but did not fair well with the surface-active solutions. The accuracy of the correlation for the liquid and solid holdups was substantially better since the absolute values of the holdups are greater. The gas holdup prediction approach proposed by Gorowara and Fan (1990) also failed because all surface-active solutions showed similar gas holdups despite presenting different dynamic surface tension behaviour.

Finally, more fundamental work is required to elucidate the complex relationship between the physical properties of a multi-component liquid, the degree of bubble coalescence and the hydrodynamic features of multiphase reactors. One potential future experiment would be to determine the effects of liquid properties and operating conditions not only on overall gas holdups, but on the bubble size distribution. Gas disengagements experiments (Lee et al., 1999) held in a bubble column would allow to associate the gas holdups to different classes of bubble size.

Nomenclature

AAD	= average absolute deviation defined in Equation (4.6), -
A_b	= bubble surface area, m^2
CMC	= critical micelle concentration, $kmol/m^3$
c_t	= transition concentration, $kmol/m^3$
D	= column diameter, m
d_b	= diameter of the bubble, m
d_p	= spherical or volume-equivalent particle diameter, m
E_M	= dilatational surface elasticity, N·s/m
Eo	= bubble Eötvös number = $g(\rho_L - \rho_g)d_b^2/\sigma$, -
F_m	= bias factor defined in Equation (4.7), -
Fr_g	= gas Froude number = U_g^2/gd_p , -
g	= acceleration due to gravity, m/s^2
H	= height of column, m
H_b	= bed height, m
k_f	= foam decay rate constant, s^{-1}
M	= bed weight of particles, kg
r	= radius of capillary, m
Re_L	= liquid Reynolds number = $\rho_L d_p U_L / \mu_L$, -
R_f	= foam retention time, s
$t_{f,(1/2)}$	= foam half-life, s
U_b	= bubble swarm velocity, m/s
U_g	= superficial gas velocity, m/s
U_L	= superficial liquid velocity, m/s
v_t	= particle terminal velocity, m/s
$v_{t\infty}$	= isolated particle terminal velocity, m/s
We_m	= modified Weber number = $U_L^2 \rho_L D_c / \sigma$, -

Greek Letters

ζ = parameter in equation (4.1), -

σ = surface tension, mN/m

$\sigma_b(0.5)$ = dynamic surface tension at 0.5 bubbles/s mN/m

$\sigma_b(4)$ = dynamic surface tension at 4 bubbles/s mN/m

σ_e = equilibrium surface tension of aqueous solution mN/m

$\varepsilon_{\text{ethanol}}$ = phase holdup for ethanol

ρ_g = gas density, kg/m³

ε_g = gas holdup, -

μ_g = gas viscosity, Pa·s

ρ_L = liquid density, kg/m³

μ_L = liquid viscosity, Pa·s

$-\Delta P$ = dynamic pressure drop = $-\Delta P_T - g\rho_L\Delta z$, Pa

ρ_p = particle density, kg/m³

ε_s = solids holdup, -

ε_{smf} = solids holdup at minimum fluidization velocity,

σ_w = surface tension of water mN/m

$\varepsilon_{\text{water}}$ = phase holdup for water

Δz = vertical distance between taps for differential pressure measurement, m

$d\sigma$ = change in surface tension mN/m

ε_{cal} = phase holdup predicted by correlation, -

ε_{exp} = phase holdup obtained experimentally, -

ε_L = liquid holdup, -

π_s = surface pressure N/m

σ_m = difference between the dynamic and equilibrium surface tension, mN/m

Φ = particle sphericity, -

ψ = coalescence percentage, %

References

- Bickerman, J.J., "Foams", Springer-Verlag, New York (1973).
- Chaudhari, R.V. and H. Hofmann, "Coalescence of Gas Bubbles in Liquids", *Reviews in Chemical Engineering*, 10, 131-190 (1994).
- Czarnecki.J, Malysa.K, Pomianowski.A, "Dynamic Frothability Index", *Journal of Colloid and interface Science*. Vol 86, No. 2, (1982).
- Davis, R.E., and Acrivos, A., "The influence of Surfactants on the Creeping Motion of Bubbles", *Chem.Eng.Sci.* 21, 681,(1966)
- Fan, L.S., "Gas-Liquid-Solid Fluidization Engineering", Butterworth Publishers, Boston, MA (1989).
- Garrett, P.R. "The Mode of Action of Antifoams", Chapter 1 in "Defoaming", P.R. Garrett, Ed., Marcel Dekker Inc., New York (1993), pp. 1-118.
- Gorowara, R.L. and L.S. Fan, "Effect of Surfactants on Three-Phase Fluidized Bed Hydrodynamics", *Ind. Eng. Chem. Res.*, 29, 882-891 (1990).
- Han, J.H., Wild, G. and S.D. Kim, "Phase Holdup Characteristics in Three-Phase Fluidized Beds", *Chem. Eng. J.*, 43, 67-73 (1990).
- Hikita, H., Asai, S., Tanigawa, K., Segawa, K. and M. Kitao, "Gas Hold-Up in Bubble Columns", *Chem. Eng. J.*, 20, 59-67 (1980).
- Huang, D.D.W., Nikolov, A. and D.T. Wasan, "Foams: Basic Properties with Application to Porous Media", *Langmuir*, 2, 672-677 (1986).
- Keitel, G. and U. Onken, "Inhibition of Bubble Coalescence by Solutes in Air/Water Dispersions", *Chem. Eng. Sci.*, 37, 1635-1638 (1982).
- Kelkar, B.G., Godbole, S.P., Honath, M.F., Carr, N.L. and W.-D. Deckwer, "Effect of Addition of Alcohols on Gas Holdup and Backmixing in Bubble Columns", *AIChE J.*, 29, 361-368 (1983).
- Koide, K, Horibe, K, Kawabata K. and I. Shigetaka, "Gas holdup and volumetric liquid-phase mass transfer coefficient in solid-suspended bubble column with draught tube", *Journal of Chemical Engineering of Japan*, 8, 248-254 (1985).

- Krishna, R., Urseanu, M.I and A.J. Dreher, "Gas Hold-up in Bubble Columns: Influence of Alcohol Addition versus Operation at Elevated Pressures", *Chem. Eng. Proc.*, 39, 371-378 (2000).
- Larachi, F., Belfares, L., Iliuta, I. and B.A. Grandjean, "Three-Phase Fluidization Macroscopic Hydrodynamics Revisited", *Ind. Eng. Chem. Res.*, 40, 993-1008 (2001).
- Lessard, R. D., & Zieminski, S. A. "Bubble coalescence and gas transfer in aqueous electrolytic solutions", *Industrial and Engineering Chemistry, Fundamentals*, 10, (1971). 260-289.
- Lee, D.J., Luo, X. and L.S. Fan, "Gas Disengagement Technique in a Slurry Bubble Column Operated in the Coalesced Bubble Regime", *Chem. Eng. Sci.*, 54, 2227-2236 (1999).
- Luo, X., Lee, D.J., Lau, R., Yang, G.Q. and L.S. Fan, "Maximum Stable Bubble Size and Gas Holdup in Slurry Bubble Columns", *AIChE J.*, 45, 665-680 (1999).
- Jamialahmadi M. and H. Müller-Steinhagen, "Effect of Alcohol, Organic Acid and Potassium Chloride Concentration on Bubble Size, Bubble Rise Velocity and Gas Hold-Up in Bubble Columns", *Chem. Eng. J.*, 50, 47-56 (1992).
- Macchi, A., "Dimensionless Hydrodynamic Simulation of High Pressure Multiphase Reactors Subject to Foaming", Ph.D. Dissertation, The University of British Columbia, (2002).
- Nacef Saci, "Hydrodynamique des lits fluidises gaz-liquide-solide" Ph.D. Dissertation, L'Institut National Polytechnique de Lorraine, (1991).
- Nacef, S., Wild, G., Laurent, A. and S.D. Kim, "Scale Effects in Gas-Liquid-Solid Fluidization", *Int. Chem. Eng.*, 32, 51-72 (1992).
- Porter, M.R., "Handbook of Surfactants", Second edition, (1994).
- Manglik R. M., Wasekar V. M and J. Zhang, "Dynamic and equilibrium surface tension of aqueous surfactant and polymeric solutions", *Experimental Thermal and Fluid Science* 25, 55-64 (2001).
- Richardson, J.F. and W.N. Zaki, "Sedimentation and Fluidization: Part 1", *Trans. Instn. Chem. Engrs.*, 32, 35-52 (1954).
- Saberian-Broudjenni, M., Wild, G., Charpentier, J.-C., Fortin, Y., Euzen, J.-P. and R. Patoux, "Contribution to the Hydrodynamic Study of Gas-Liquid-Solid Fluidized Bed Reactors", *Int. Chem. Eng.*, 27, 423-440 (1987).

- Schramm, L.L. and F. Wassmuth, "Foams: Basic Principles", Chapter 1 in "Foams: Fundamentals and Applications in the Petroleum Industry", Adv. in Chem. Series 242, L.R. Schramm, Ed., American Chemical Society, Washington D.C. (1994), pp. 3-47.
- Shah, Y.T, Joseph, S., Smith, D.N. and J.A. Ruether, "On the Behavior of the Gas Phase in a Bubble Column with Ethanol-Water Mixtures", Ind. Eng. Chem. Process Des. Dev., 24, 1140-1148 (1985).
- Sultana R. S, Afacan A. and K. T. Chuang , "Prediction of Gas Hold-up in a Bubble Column Filled with Pure and Binary Liquids", The Canadian Journal of Chemical engineering, 80, (2002).
- Tomasic, V., Stefanic, I., Filipovic-Vincekovic, N., "Adsorption, association and precipitation in hexadecyltrimethylammonium bromide/sodium dodecyl sulphate mixtures", Colloid Polym Sci 277:153-163 (1999).
- Vial, C., Poncin, S., Wild, G. and N. Midoux, "A Simple Method for Regime Identification and Flow Characterisation in Bubble Columns and Airlift Reactors", Chem. Eng. Proc., 40, 135-151 (2001).
- Wild, G. and S. Poncin, "Hydrodynamics", Chapter 1 in "Three-Phase Sparged Reactors", K.D.P Nigam and A.Shumpe, Eds., Gordon and Breach Publishers, Netherlands (1996), pp. 11-112.
- Wilkinson, P.M., Spek, A.P. and L.L. van Dierendonk, "Design Parameters Estimation for Scale-Up of High-Pressure Bubble Columns", AIChE J., 38, 544-554 (1992).
- Zahradnik, J., Fialova, M. and V. Linek, "The Effects of Surface-Active Additives on Bubble Coalescence in Aqueous Media", Chem. Eng. Sci., 54, 4757-4766 (1999).
- Zhang J.P., Epstein N., Grace J.R. and Zhu J., "Minimum liquid fluidization velocity of gas-liquid fluidized beds". Trans IChemE, (73): 347-353 (1995).